BOSTON UNIVERSITY

COLLEGE OF ENGINEERING

Senior Honors Thesis

QUANTUM SIMULATION OF BENZENE USING DIRECTIONALLY UNBIASED LINEAR-OPTICAL MULTIPORTS

by

SONAM K. GHOSH

B.S., Boston University, 2018

Submitted in partial fulfillment of the

requirements for the degree of

Bachelor of Science

2018

Approved by

First Reader

Alexander V. Sergienko, PhD
Professor of Electrical and Computer Engineering
Professor of Physics

Second Reader

Tali Moreshet, PhD
Professor of Electrical and Computer Engineering

Third Reader

Alan Pisano, PhD
Associate Professor of Electrical and Computer Engineering

In less than ten years
quantum computers will begin to outperform every day computers,
leading to breakthroughs in artificial intelligence,
the discovery of new pharmaceuticals and beyond.
The very fast computing power given by quantum computers
has the potential to disrupt traditional businesses
and challenge our cyber-security
Businesses need to be ready for a quantum future because it's coming

Jeremy O'Brien, UNSW Ph.D & Quantum Optics/Information Science Researcher ("Quantum computing is coming- are you prepared for it", 2016)

Acknowledgments

I would like to thank Alexander Sergienko, David Simon, and Shuto Osawa for guiding me through the entire journey of Quantum Computing from the theoretical to the experimental and for providing me this fulfilling opportunity. I would like to thank Professor John Butler of the BU Physics Department for his excellent Modern Physics course that inspired to go down the road of pursuing a deeper background in Physics which lead to obtaining a minor in Physics. I would like to thank my AP Physics B high school teacher Richard Newton for channeling and generating an enormous passion for Physics and spurring me towards Engineering during my senior year in High School. I would like to thank my parents and my sister for being there for support and encouragement every step of the way. Lastly, I want to thank my friends from high schools and BU for trying their best to keeping me sane and entertained through this journey. Quick shoutout to my fellow physics partner-in-crime and friend from high school, Nick Russo for enlightening late night science discussion!

Sonam K. Ghosh

Boston, MA

April, 2018

QUANTUM SIMULATION OF BENZENE USING DIRECTIONALLY UNBIASED LINEAR-OPTICAL MULTIPORTS

SONAM K. GHOSH

ABSTRACT

Quantum Computing offers a novel approach to processing new information using the principles of Quantum Mechanics. Quantum Computing allows us to run new types of algorithms at quick and efficient speeds which can lead to breakthroughs in cryptography, machine learning, or drug discovery.

Quantum Computing allows for the potential of running new types of algorithms and simulations at faster and efficient speeds than classical computing. Applications of quantum computing encompass a wide array of fields from machine learning to chemistry. Quantum Computation can be done through various techniques such as superconducting circuits, cold-atoms, and photonic elements. In this thesis, applications of linear-optical quantum computing will be employed. Simple quantum simulations are utilized to model the behavior of a complex physical system such as a molecular system which in the scope of this work was a benzene molecule. The benzene molecule is modeled optically through an arrangement of connected directionally-unbiased optical triports. The Hamiltonian which governs the energy dynamics of the system is determined for the system in a specific case and then later on a generalized model is derived. The eigenvalues and eigenvectors which represent the energies and states of the system are numerically and analytically determined and compared to an established approximated model of Benzene. By adjusting triport phase angles, the model may be adjusted to closely match the molecular Benzene model.

Contents

1 Introduction **1**

1.1 Context and contents of this thesis 1

1.2 Structure of this thesis 2

1.3 Background 3

1.3.1 Quantum Mechanics 3

1.3.2 Quantum Optics 11

1.3.3 Quantum Information/Computing 13

1.3.4 Linear Optical Quantum Computing 16

1.3.5 Quantum Walks 19

1.4 Purpose of this Project 25

2 Motivation **26**

2.1 Concept Development 26

3 System Description **28**

3.1 Experiemental Abstraction 28

3.2 Laboratory Setup of Single Optical Triport 32

3.3 Software Implementation 33

4 Optical Benzene Model **34**

4.1 Basis Formulation 34

4.2 States of the System 35

4.2.1 Triport Representation 35

4.2.2 Unit Cell Representation 35

4.3 Directionally-Unbiased Optical Three-Ports . . . 35
4.4 The Full General Model . . . 37
4.4.1 System Interactions . . . 37
4.4.2 Transition Amplitudes . . . 38
4.4.3 Full Unitary Matrix Formulation . . . 39
4.4.4 Full Hamiltonian Model . . . 40
4.5 Reduced General Model without Direction of Movement . . . 41
4.5.1 Projection Operator . . . 41
4.5.2 Reduced Hamiltonian Model . . . 41

5 Eigendecomposition of the System **42**

5.1 Eigenvalues of Full Hamiltonian . . . 42
5.2 Eigenstates of Full Hamiltonian . . . 42
5.3 Eigenanalysis for $\phi = \pi/2$ . . . 43
5.3.1 Parameter Values . . . 43
5.3.2 Matrix Block Values . . . 43
5.3.3 Eigenvalues . . . 44
5.3.4 Eigenstates . . . 44
5.3.5 Qualitative Description . . . 45
5.4 Eigenanalysis for $\phi = 3\pi/2$ . . . 45
5.4.1 Parameter Values . . . 45
5.4.2 Matrix Block Values . . . 45
5.4.3 Eigenvalues . . . 46
5.4.4 Eigenstates . . . 49
5.4.5 Qualitative Description . . . 51
5.5 Eigenspectrum for Full Hamiltonian . . . 51
5.5.1 Discussion . . . 52

5.6 Eigenspectrum of Reduced Hamiltonian 54
5.6.1 Discussion 54

6 Conclusions **58**

6.1 Summary of Work and future directions 58

A Appendices **60**

A.1 Huckel 60
A.2 Matrix Logarithm 64
A.3 Engineering Requirements 65

References **68**

Thank You **70**

List of Tables

5.1 Corresponding Eigenstates to the Eigenvalues for $H(\pi/2)$ 44

List of Figures

1·1 Bloch sphere representation of a qubit 14

1·2 Linear Quantum Gate with N input and output ports ($N = 3$ in figure) 18

1·3 MATLAB Plot of Eq. 1.74 for $n = 100, p = \frac{1}{2}$. The probability of finding the particile at position $k = 0$ is equal 0.0795. 21

1·4 Probability distribution of 100 steps DTQW using the above defined coined and translational operators 23

3·1 The Directionally-Unbiased Optical Three port. The thin blue rectangles represent the directionally-unbiased beam splitters. The colored rectangles represent the mirror units which contain a phase shifter and a mirror. 29

3·2 The Mirror Unit which consists of a phase shifter and a mirror. The distance between each beam splitter and the adjacent mirror is half the distance d between one beam splitter and the other. The phase shifter will be helpful in controlling the phase of the photons and interference of photon paths. 30

3·3 The Unit Cell of two directionally-unbiased triports connected to represent a double bond of a benzene system and the other end representing a single bond. Three of these unit cells will make up the optical benzene setup. S (single-bond state) and D (double-bond state) will later on be used to represent in bond states of the cell in our Hamiltonian model. 31

3·4 Side by Side of a Benzene molecule (C_6H_6) with the abstraction of our Optical Benzene molecule. Photons injected into the optical system will undergo quantum random walks around the system analagous to the electron movement in the aromatic ring of a Benzene molecule . . 31
3·5 Optical Schematic of a Single Optical Triport 32

5·1 Probability Amplitudes as a function of the state $|B, M, n\rangle$ of the periodic behaviour Eigenstates for the associated Eigenvalues for the full Hamiltonian evaluated with a multiport phase angle of $3\pi/2$ 50
5·2 Probability Amplitudes as a function of the state $|B, M, n\rangle$ of the mixed behaviour Eigenstates for the associated Eigenvalues for a Hamiltonian evaluated with a multiport phase angle of $3\pi/2$ 51
5·3 Eigenvalue/Eigenenergy $E_i(\phi)$ spectrum of the full 12 by 12 Hamiltonian (B,M,n) as a function of the multiport phase angle ϕ 52
5·4 The eigenvalues the system converges as the multiport phase angle $\phi \to \pi/6$ 53
5·5 Eigenvalue/Eigenenergy spectrum of the projected Hamiltonian (B, n) as a function of the multiport phase angle ϕ 54
5·6 Probability Amplitude as a function of the state $|B, M, n\rangle$ of the Periodic Eigenstates for the associated Eigenvalues for a Hamiltonian solved with a multiport phase angle of $\pi/6$ 56
5·7 Energy Comparison of the Huckel Model of Benzene versus the Optical Benzene model under a phase angle of $11\pi/6$ 57

List of Abbreviations

H.c.	.....	Hermitian conjugate
QIP	.....	Quantum information processing
LOQC	.....	Linear Optical Quantum Computing
PDF	.....	Probability Distribution Function
$\mathbb{R}^2$	.....	the Real plane
$\mathbb{C}$	.....	The Complex plane
$\mathbb{Z}$	.....	Real Numbers
MO	.....	Molecular Orbitals

Chapter 1

Introduction

1.1 Context and contents of this thesis

Quantum Computing offers us powerful machines that offer a novel approach to processing new information based on the principles of Quantum Mechanics. By utilizing Quantum Mechanical principles, quantum computing allows to run new types of algorithms at fast and efficient speeds which can lead to breakthroughs in cryptography, machine learning, or drug discovery. In 1936, Alan Turing developed the model for a programmable computer which would be known as the *Turing Machine* and later on developed the theory of the *Universal Turing Machine* which can simulate any Turing Machine. If an algorithm can be performed on any piece of hardware, then there is an equivalent algorithm for the Universal Turning Machine which can perform the same exact same task (Turing, 1937). This concept would give rise to the concept of Quantum Simulations. In 1982, Richard Feynmann suggested building computers based on the principles of Quantum Mechanics to avoid difficulties in solving two important difficult algorithms - Shor's Algorithm (finding prime factors of any integer and solving the discrete logarithm) and Grover's Algorithm (fast search algorithm on unstructured search space) (Feynman, 1982).

Current approaches to Quantum computation rely on the principles of superposition and entanglement for an edge over classical computing. There are several requirements for a physical implementation of a quantum computer such as a defined extendable qubit array for stable memory, feasible state preparation for the initial

state, long decoherence time, a universal set of gate operations and capability for single quantum measurements (Nielsen and Chuang, 2011).

One practical system to simulate via quantum computation are molecular systems. Computational Chemistry aids in research and development in drug and materials discovery which require demanding computational tools and power. The inherent quantum nature of molecular systems make it an excellent candidate to test quantum computing on as well as provide accurate modeling to researchers. Many problems in computational chemistry exist such as prediction of chemical reactions and the description of excited electronic states, transition states, and ground states of transition metal complexes. Using current computational methods require computational resources that scale exponentially with the system size. The ability to tap into the properties of quantum entanglement and superposition will greatly help computational speed up as now we will be able to deal with multiple variables simultaneously with quicker computational time.(Aspuru-Guzik and Walther, 2012).

1.2 Structure of this thesis

This structure is divided into 6 chapters. The rest of this chapter will focus on the needed mathematical, scientific and notation knowledge of Quantum Mechanics, Quantum Computing, Linear Optical Quantum Computing, and Quantum Walks followed by the purpose of the entire thesis. Chapter 2 will provide a description on the Motivation of this work. Chapter 3 will provide a System Description describing the abstraction, software implementation, and experimental setup. Chapter 4 will define out the Optical Benzene System mathematically. Chapter 5 will discuss the analysis of the Eigenenergies and Eigenstates of the System and Chapter 6 will finally wrap things up. The Appendix will contain information on the conventional Benzene

molecule and the Matrix Logarithm operation.

1.3 Background

1.3.1 Quantum Mechanics

The language of Quantum Physics must first be understood to go about with any sort of work involving Quantum Algorithms or Quantum Chemistry and beyond. In this section, a brief introduction to the mathematical formalism and physical meaning behind Quantum Mechanics will be defined and given. A very powerful formalism to put Quantum Mechanics in a simplistic way is through Dirac Formalism which is very important to applications in Quantum Mechanics such as quantum information. The mathematics of Quantum Mechanics is described via Linear Algebra. Let us start with some important details:

1. A vector will be denoted as $|n\rangle$ or $\langle n|$ (More on this notations meeting later).
2. Vectors are complex and thus can have imaginary components.
3. Vectors may have infinite components and have the possibility of having a continuum of components.
4. The state of a system is described by a vector
5. Observables (measurable things) correspond to operators which perform a linear transformations on vectors.
6. The principle of a superposition allows for the linear combination of two wavefunctions to be a possible wavefunction for the system.

Dirac Notation

A vector or state will be denoted as $|\psi\rangle$ which is known as the "ket"-vector or as a

"bra"-vector denoted as $\langle\psi|$ (Note that the bra is the complex conjugate transpose of the ket). A bra and ket together together provides a braket $\langle n|m\rangle$ which denotes the scalar (inner) product of the vectors $|n\rangle$ and $|m\rangle$ (Note that $\langle n|m\rangle = \langle m|n\rangle^*$).

Vector Space

The vector space contains scalars and vectors. One can define a new state ψ with the superposition of some states α and β multiplied by scalar constants a, b respectively:

$$|\psi\rangle = a\,|\alpha\rangle + b\,|\beta\rangle \tag{1.1}$$

a and b must follow the normalization property of Probability Theory:

$$|a|^2 + |b|^2 = 1 \tag{1.2}$$

A vector may also be expanded as a set of linearly independent basis vectors $|e_i\rangle\,, i = 1, 2, .., n$:

$$|\alpha\rangle = \sum_{i=1}^{n} a_i\,|e_i\rangle \tag{1.3}$$

Where a_i are complex scalars and denoted as the components of the vector and n to be the dimension of the vector space. If we describe e_i to be an orthonormal basis:

$$\langle e_i|e_j\rangle = \delta_{i,j} \tag{1.4}$$

The components of the vector $|\alpha\rangle$ are given by:

$$a_i = \langle e_i|\alpha\rangle \tag{1.5}$$

And the inner product of α and β are given by:

$$\langle\alpha|\beta\rangle = \sum_{i=1}^{n} a_i^* b_i \tag{1.6}$$

And the norm of the vector α is given by:

$$\langle\alpha|\alpha\rangle = \sum_{i=1}^{n} a_i^* a_i \tag{1.7}$$

Linear Transformations/Operators

An Operator $\hat{O}$ will apply an linear transformation to a vector $|\alpha\rangle$ to get a new transformed vector $|\alpha'\rangle = \hat{O}\,|\alpha\rangle$ and obeys linearity conditions:

$$\hat{O}(a\,|\alpha\rangle + b\,|\beta\rangle) = a\hat{O}\,|\alpha\rangle + b\hat{O}\,|\beta\rangle \tag{1.8}$$

The action of an operator $\hat{O}$ on an arbitrary vector can be obtained from the action on the basis states which will now be denoted as $|i\rangle$:

$$\hat{O}\,|j\rangle = \sum_{i=1}^{n} O_{ij}\,|i\rangle \tag{1.9}$$

$$O_{ij} = \langle i|\hat{O}|j\rangle \tag{1.10}$$

O_{ij} is known as the component or matrix element of the operator $\hat{O}$ which forms a $n \times n$ matrix.

Hermitian Transformations

If $\hat{O}$ is an operator, then the hermitian conjugate operator $\hat{O}^\dagger$ is given by:

$$\langle\alpha|\hat{O}^\dagger|\beta\rangle = \langle\beta|\hat{O}|\alpha\rangle^* \tag{1.11}$$

A very important concept in Quantum mechanics involve Hermitian Conjugates equal the operator of itself:

$$\hat{O} = \hat{O}^\dagger \tag{1.12}$$

These operators are said to be *hermitian*

Eigenvalues/Eigenvectors

Eigenvalue/Eigenvector problems show up all throughout Quantum Mechanics:

$$\hat{O}\left|n\right\rangle = \lambda\left|n\right\rangle \tag{1.13}$$

Where λ is the eigenvalue of the system and the vector $|n\rangle$ represent the eigenstates/eigenvectors of the system.

If a operator $\hat{O}$ is hermitian, the following properties hold:

1. All eigenvalues are real
2. Eigenvectors corresponding to different eigenvalues are orthongonal
3. The eigenvectors span the vector space

The Operator Identity which is very useful due to its ability to be inserted anywhere is as follows:

$$I = \sum_{i=1}^{n} \left|i\right\rangle \left\langle i\right| \tag{1.14}$$

Using this identity operator, we can derive the components of a operator $\hat{O}$ in the basis $\{|i\rangle\}$ as the following:

$$\hat{O} = \hat{I}\cdot\hat{O}\cdot\hat{I} = \sum_{i,j} \left|i\right\rangle \left\langle i|\hat{O}|j\right\rangle \left\langle j\right| = \sum_{i,j} \left|i\right\rangle O_{ij} \left\langle j\right| \tag{1.15}$$

Time Evolution/Unitary Transformations

Often for experiments and simulations, one would like develop an eigenfunction expansion to provide the means to seeing the time evolution of a wavestate/wavefunction $|\psi\rangle$. One may move a state forward in time by applying a time evolution operator. Where the state as a function of time after applying the time-evolution operator is given by:

$$\left|\psi(t)\right\rangle = \hat{U}\left|\psi(0)\right\rangle \tag{1.16}$$

Where the time operator $\hat{U}$ is defined as

$$\hat{U} = e^{-i\hat{H}t/\hbar} \tag{1.17}$$

Applying the Identity operator on the time evolved state and defining $|i\rangle$ as the eigenstates of the Hamiltonian $\hat{H}$ we obtain the following expression:

$$|\psi(t)\rangle = e^{-i\hat{H}t/\hbar} \sum_i |i\rangle \langle i|\psi(0)\rangle = \sum_i |i\rangle \langle i|\psi(0)\rangle e^{-iE_i t/\hbar} \tag{1.18}$$

The time evolution operator is known as a *Unitary operator*. Unitary operators are defined as transformations which preserve the scalar product:

$$\langle\phi|\psi\rangle = \langle\hat{U}\phi|\hat{U}\psi\rangle = \langle\phi|\hat{U}^\dagger\hat{U}\psi\rangle = \langle\phi|\psi\rangle \rightarrow \hat{U}\hat{U}^\dagger = I \tag{1.19}$$

Change of Basis

Change of basis under Dirac Formalism is useful when redefining states or making the matrix of a system simpler in a QM setup. Once again the Identity Operator will come in handy for making this setup.

Let $|a_i\rangle$ and $|b_i\rangle$ $(i = 1, 2, ..., n)$ be two sets of normalized basis vectors. Two resolutions will fall out of the identity operator:

$$\hat{I} = \sum_i |a_i\rangle \langle a_i| = \sum_i |b_i\rangle \langle b_i| \tag{1.20}$$

Now we derive a relation that relates two vector sets:

$$|a_i\rangle = \sum_j |b_j\rangle \langle b_j|a_i\rangle \tag{1.21}$$

A vector $|\psi\rangle$ can be expanded as:

$$|\psi\rangle = \sum_i |a_i\rangle \langle a_i|\psi\rangle = \sum_i |b_i\rangle \langle b_i|\psi\rangle \tag{1.22}$$

With components related as:

$$\langle a_i|\psi\rangle = \sum_j \langle a_i|b_j\rangle \langle b_j|\psi\rangle \tag{1.23}$$

We can rewrite this in matrix notation as:

$$\psi^{(a)} = \mathbf{S}\psi^{(b)} \tag{1.24}$$

Where $\psi^{a/b}$ is the vector with elements $\langle a_i/b_i|\psi\rangle$ and the matrix $\mathbf{S}$ with elements $S_{ij} = \langle a_i|b_j\rangle$

For an operator $\hat{O}$ we get the following expression:

$$\langle a_i|\hat{O}|a_j\rangle = \sum_{k,m} \langle a_i|b_k\rangle \langle b_k|\hat{O}|b_m\rangle \langle b_m|a_i\rangle \tag{1.25}$$

In matrix notation the above epxression becomes:

$$\boldsymbol{O}^{(a)} = \boldsymbol{S}\,\boldsymbol{O}^{(b)}\,\boldsymbol{S}^{-1} \tag{1.26}$$

Where $\boldsymbol{S}^{-1}$ has components $S^{-1}_{ij} = \langle b_i|a_j\rangle$. This transformation allows for the diagonalization of the matrix $\boldsymbol{O}^{(b)}$ by finding a transformation matrix $\boldsymbol{S}$ such that $\boldsymbol{O}^{(a)}$ is diagonal is equivalent to transforming a basis consisting of the eigenvectors of an operator $\hat{O}$.

Statistical Interpretation

A quantum mechanical system is described by a vector $|\psi\rangle$ in a Hilbert space $\mathcal{H}$ where every vector in $\mathcal{H}$ describes a possible state for the system.

Every observable (measurable quantity) A corresponds to a hermitian operator $\hat{A}$ acting on the vectors in $\mathcal{H}$.

The expectation value for an observable A is

$$\langle A\rangle = \frac{\langle\psi|\hat{A}|\psi\rangle}{\langle\psi|\psi\rangle} = \langle\psi|\hat{A}|\psi\rangle \tag{1.27}$$

A measurement of an observable A gives one of the eigenvalues λ_i of the hermitian operator $\hat{A}$ with eigenvectors $|n_i\rangle$.

Given $|\psi\rangle = \sum_i |n_i\rangle \langle n_i|\psi\rangle$, then the probability P_i to get λ_i after a measurement is given by:

$$P_i = \frac{|\langle n_i|\psi\rangle|^2}{\langle\psi|\psi\rangle} = |\langle n_i|\psi\rangle|^2 \tag{1.28}$$

Note the normalization $\langle\psi|\psi\rangle = 1$.

After measurement, the wavefunction collapses into the eigenstate/eigenvector $|n_i\rangle$ corresponding to the measured eigenvalue λ_i. Repeated measurement of A after this measurement will keep giving the same measurement λ_i with probability 1.

Ladder Operators

In the context of Linear Algebra but specifically Quantum Mechanics, ladder operators are operators (matrices) that can increase or decrease the eigenvalue of another operator or state. There are two types of ladder operators - the raising operator (or creation operator) and the lowering operator (annihilation or destruction operator). They are frequently used in Quantum Mechanics , especially in the harmonic oscillator systems, quantum optical systems, and angular momentum.

Suppose you have two operators N and A and a constant γ with the following commutation relation:

$$[N, A] = \gamma A \tag{1.29}$$

Operator N has an eigenstate $|n\rangle$ with eigenvalue n that satisfies the eigenvalue-eigenvector problem:

$$N|n\rangle = n|n\rangle \tag{1.30}$$

Then the operator A acts on the eigenstate $|n\rangle$ such that the eigenvalue is shifted by the constant scalar γ

$$NA|n\rangle = (AN + [N, A])|n\rangle \tag{1.31}$$

$$= AN|n\rangle + [N, A]|n\rangle \tag{1.32}$$

$$= An|n\rangle + \gamma A|n\rangle \tag{1.33}$$

$$= (n + \gamma)A|n\rangle \tag{1.34}$$

Therefore, since $|n\rangle$ is an eigenstate of N then $A|n\rangle$ is an eigenstate of N with an eigenvalue of $n + \gamma$. In other words, the operator A is a raising operator if γ is real and positive and a lowering operator if γ is is real and negative.

Let us define some basic raising and lowering operators (2D) in their matrix representation and defined in terms of the pauli matrices which are as follows:

$$\sigma_1 = \sigma_x = \begin{pmatrix} 0 & 1 \\ 1 & 0 \end{pmatrix}, \sigma_2 = \sigma_y = \begin{pmatrix} 0 & -i \\ i & 0 \end{pmatrix}, \sigma_3 = \sigma_z = \begin{pmatrix} 1 & 0 \\ 0 & -1 \end{pmatrix} \tag{1.35}$$

The raising (creation) operator:

$$a^\dagger = a_+ = \begin{pmatrix} 0 & 0 \\ 1 & 0 \end{pmatrix} = \frac{1}{2}(\sigma_1 - i\sigma_2) \tag{1.36}$$

The lowering (annihilation or destruction) operator:

$$a = a_- = \begin{pmatrix} 0 & 1 \\ 0 & 0 \end{pmatrix} = \frac{1}{2}(\sigma_1 + i\sigma_2) \tag{1.37}$$

The number operator (particle or one) operator:

$$n = \begin{pmatrix} 0 & 0 \\ 0 & 1 \end{pmatrix} = a^\dagger a = \frac{1}{2}(1 - \sigma_3) \tag{1.38}$$

The other number operator (hole or zero) operator:

$$h = \bar{n} = \begin{pmatrix} 1 & 0 \\ 0 & 0 \end{pmatrix} = aa^\dagger = \frac{1}{2}(1 + \sigma_3) \tag{1.39}$$

The number operators follow the following anticommutation relation algebraically (produces the identity operator):

$$a^\dagger a + aa^\dagger = n + h = \mathbf{1} \tag{1.40}$$

1.3.2 Quantum Optics

Quantum optics is an area of physics that encompasses Quantum Mechanics, Electromagnetic Theory, and Photonics in order to investigate the phenomena involving light and its interaction with matter such as atoms and molecules. In the context of this thesis and further work it is important to understand the quantum mechanical behavior of optical equipment such as beam splitters which split incident light into two or more beams.

Quantum Mechanical Description of Beam Splitters

Beam splitters are important in quantum mechanics, especially in quantum information where beam splitters are important for teleportation, bell measurements, and entanglement.

Suppose you have two electric fields E_1 and E_2 enter the beam splitter at separate ports respectively. The first field evolves with the following relation: $E_1 \to tE_3 + rE_4$ and the second field evolves with the the following relation: $E_2 \to rE_3 + tE_4$ where t, r are the transmission and reflection coefficients for the beam splitter.

Assuming the beamsplitter is lossless or approximately lossless, it can be deduced that the transformation undergone in the relations above is unitary which gives rise

to the following relations

$$|t|^2 + |r|^2 = 1 \tag{1.41}$$

$$r^* t + r t^* = 0 \tag{1.42}$$

Now represent the fields as raising and lowering operators. Let the two input fields be denoted by the lowering operators a_0, a_1 and the two output fields be denoted by the lowering operators a_2 and a_3 (Gerry and Knight, 2005). The transformation matrix of this relation is denoted below:

$$\begin{pmatrix} a_2 \\ a_3 \end{pmatrix} = \begin{pmatrix} t' & r \\ r' & t \end{pmatrix} \begin{pmatrix} a_0 \\ a_1 \end{pmatrix} \tag{1.43}$$

The transformation matrix above must obey the following commutation relations:

$$[a_i, a_j^\dagger] = \delta_{ij} \tag{1.44}$$

$$[a_i, a_j] = 0 \tag{1.45}$$

The matrix must also follow Eq. (1.41) and Eq. (1.42) and $|r'| = |r|$ and $|t'| = |t|$. Utilizing a 50-50 beam splitter, the reflected and transmitted light is offset by a phase of $e^{\pm i\pi/2} = \pm i$. Which gives rise to the following relations for the output lowering operators.

$$a_2 = \frac{1}{\sqrt{2}}(a_0 + i a_1), a_3 = \frac{1}{\sqrt{2}}(i a_0 + a_1) \tag{1.46}$$

This transformation matrix can be represented as a unitary transformation given as

$$\hat{U} = e^{i\frac{\pi}{4}(a_0^\dagger a_1 + a_0 a_1^\dagger)} \tag{1.47}$$

$$\begin{pmatrix} a_2 \\ a_3 \end{pmatrix} = \hat{U}^\dagger \begin{pmatrix} a_0 \\ a_1 \end{pmatrix} \hat{U} \tag{1.48}$$

1.3.3 Quantum Information/Computing

Introduction to Quantum Computing

Classical computers are built upon the concept of a *bit*. Quantum computation and information are build upon the *qubit* (quantum bit) the analog to the classical bit. The two possible states are based on the computational basis states of $|0\rangle$ and $|1\rangle$. As opposed to classical bits where a bit can either take a 0 or 1, a qubit can take another state formed from a superposition of states given as:

$$|\psi\rangle = \alpha\,|0\rangle + \beta\,|1\rangle \tag{1.49}$$

Where α , β are complex numbers. When a qubit is measured, one will either get the state $|0\rangle$ with probability $|\alpha|^2$ or state $|1\rangle$ with probability $|\beta|^2$, (Note the constants must follow the normalization condition $|\alpha|^2+|\beta|^2 = 1$, as the sum of the probabilities must add up to 1). Generally, the state of a qubit can be described as a unit vector in two-dimensional complex vector space.

There are many physical ways to realize qubits such as:

1. Two different polarizations of a photon
2. Alignment of Nuclear Spin in a uniform magnetic field
3. Two states of an electron orbiting a single atom.

A useful geometric representation of the qubit can be that of a spinor:

$$|\psi\rangle = e^{i\gamma}\Big(\cos\frac{\theta}{2}\,|0\rangle + e^{i\varphi}\sin\frac{\theta}{2}\,|1\rangle\Big) \tag{1.50}$$

Where θ, φ, γ are real numbers. The relative phase γ doesn't give any observable effects so it can be neglected and the state can be boiled down to:

$$|\psi\rangle = cos\frac{\theta}{2}\,|0\rangle + e^{i\varphi}\sin\frac{\theta}{2}\,|1\rangle\,. \tag{1.51}$$

The state of a single qubit can be visualized by the three-dimensional space of a Bloch Sphere (shown below). Note there is no generalization for a Bloch sphere for multiple qubits. If there were two qubits, then a four computational basis is form of the states

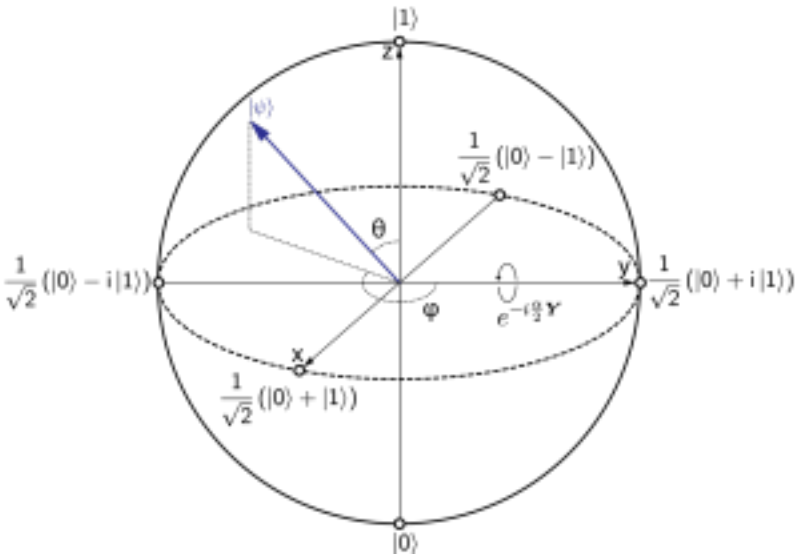

Figure 1·1: Bloch sphere representation of a qubit

$|00\rangle, |01\rangle, |10\rangle, |11\rangle$. The state vector representing a possible superposition of these four states is given by:

$$|\psi\rangle = \alpha\,|00\rangle + \beta\,|01\rangle + \xi\,|10\rangle + \eta\,|11\rangle \tag{1.52}$$

For a two qubit system, one can measure a subset of qubits, and so the probability of finding say just the first qubit gives 0 with probability $|\alpha|^2 + |\beta|^2$, providing a post measurement state of:

$$|\psi'\rangle = \frac{\alpha\,|00\rangle + \beta\,|01\rangle}{\sqrt{|\alpha|^2 + |\beta|^2}} \tag{1.53}$$

The Bell state (EPR Pair) will be useful in Quantum Information especially for concepts like teleportation and superdense coding:

$$\frac{|00\rangle + |11\rangle}{\sqrt{2}} \tag{1.54}$$

Quantum Gates

In order to do qubit operations, the quantum analogue for classical wires and logic gates are needed to transport information and manipulate information. For example the NOT Gate which flips a bit into the opposite, would do the following operation on a qubit in the quantum analogue:

$$\alpha\,|0\rangle + \beta\,|1\rangle \rightarrow \alpha\,|1\rangle + \beta\,|0\rangle \tag{1.55}$$

One can define several gate operations out of the pauli spin matrices $\{\sigma_x, \sigma_y, \sigma_z\}$. For example the quantum NOT gate can be made out of the σ_x matrix defined as the matrix X, Note that quantum gates require the constraint of that they must be unitary ($A^\dagger A = I$):

$$X = \begin{bmatrix} 0 & 1 \\ 1 & 0 \end{bmatrix} \tag{1.56}$$

The Z gate only acts on flipping the sign of the $|1\rangle$ state to $-\,|1\rangle$, leaving $|0\rangle$ unchanged is given as the σ_z matrix:

$$Z = \begin{bmatrix} 1 & 0 \\ 0 & -1 \end{bmatrix} \tag{1.57}$$

Another important gate operation is the Hadamard gate also known as the *square root of NOT* gate. The Hadamard Gate turns a $|0\rangle$ into $(|0\rangle + |1\rangle)/\sqrt{2}$ and turns $|1\rangle$ into $(|0\rangle - |1\rangle)/\sqrt{2}$. (Note applying a Hadamard gate twice to a state does nothing to it as $H^2 = I$:

$$H = \frac{1}{\sqrt{2}} \begin{bmatrix} 1 & 1 \\ 1 & -1 \end{bmatrix} \tag{1.58}$$

In the bloch sphere representation, the hadamard operation would correspond to rotations around the different axes which in this case causes 180 degree rotation around x and a 90 degree rotation around y.

Other Single Qubit Operation gates include the Y-gate, Phase Gate S, and $\pi/8$ gate T given as the following:

$$Y = \begin{bmatrix} 0 & -i \\ i & 0 \end{bmatrix}, S = \begin{bmatrix} 1 & 0 \\ 0 & i \end{bmatrix}, T = \begin{bmatrix} 1 & 0 \\ 0 & e^{i\pi/4} \end{bmatrix} \tag{1.59}$$

The next important computing operation is of Controlled operations such as "If this then do that". The controlled-NOT gate or CNOT for short is a quantum gate with two input qubits, known as the *control* qubit and *target* qubit. The CNOT operation is given by $|c\rangle |t\rangle \rightarrow |c\rangle |t \oplus c\rangle$. For example, if the control qubit is set to $|1\rangle$ then the target qubit is flipped, otherwise the target qubit is left alone. The matrix representation of CNOT is given by:

$$CNOT = \begin{bmatrix} 1 & 0 & 0 & 0 \\ 0 & 1 & 0 & 0 \\ 0 & 0 & 0 & 1 \\ 0 & 0 & 1 & 0 \end{bmatrix} \tag{1.60}$$

Next in the context of this thesis, we will discuss the Linear Optical Quantum Computing.

1.3.4 Linear Optical Quantum Computing

Introduction to LOQC

Quantum Computing via Linear Optics has the edge that photons which can be used for quantum information storage is potentially free from decoherence as the information in a photon tends to stay where it is; however, the problem of photons being unable to interact with each other which makes it difficult to apply gate operations. In order to create an optical quantum computer, one must come up with a way to introduce interaction between photons (Kok et al., 2007). For example, one may introduce large cross-Kerr nonlinearities to induce a single photon CNOT operation. Another method is making projective measurements with photo-detectors; however,

optical quantum gates are probabilistic (currently due to this nature, the gate can fail and destroy information in the computation).

The building blocks of linear optics include beam splitters, half wave plates, quarter wave plates, phase shifters, and other optical equipment. Building a network of these optical components will suffice a universal quantum computing systems; however, the size of such a network grows rapidly.

Linear Optical Multiports

Multiports are a generalization of a optical device made out of beam splitters and phase shifters. In the case of LOQC, bosonic qubits are utilized which are defined by the states of optical modes known as Fock states. Using the basis for a Quantum Harmonic Oscillator and electromagnetic field quantization, define the well known raising and lowering operators:

$$a\,|n\rangle = \sqrt{n}\,|n-1\rangle \tag{1.61}$$

$$a^\dagger\,|n\rangle = \sqrt{n+1}\,|n+1\rangle \tag{1.62}$$

n refers to the number of photons in a mode and we assert the condition of $a\,|0\rangle = 0$ due to no eigenstate of lower energy than the ground state. In order to generate a Fock state of the kth mode $|n_k\rangle$ from the vacuum, apply the ladder operators several times.

$$|n_k\rangle = \frac{a_k^\dagger}{\sqrt{n_k!}}\,|0\rangle \tag{1.63}$$

Given a linear quantum gate with N inputs, one may describe the model classically as a relation between outgoing and incoming waves (Adami and Cerf, 1999).

$$b_i = \sum_{j=1}^{N} \Lambda_{ij} q_j \tag{1.64}$$

where $b_i(q_i)$ are the complex amplitudes of the outgoing (incoming) waves and Λ_{ij} is the unitary matrix transformation from port i to port j which depends on the chosen linear optical element

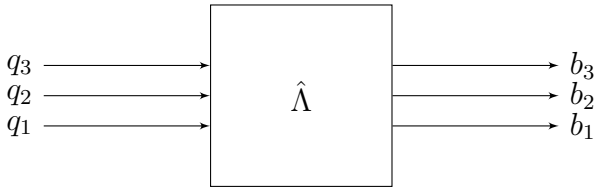

Figure 1·2: Linear Quantum Gate with N input and output ports ($N = 3$ in figure)

Quantum mechanically, q_i and b_i become operators that satisfy the commutation relations in Eq. (1.44) and Eq. (1.45). Given N input ports, the basis can be defined as a product of number states for each mode:

$$|n_N\rangle \otimes \cdots \otimes |n_2\rangle |n_1\rangle = |n_N \dots n_2 n_1\rangle \tag{1.65}$$

It is impossible to know the path taken by a photon within a multiport device, one must add up all the accumulated phases over all the paths inside the system and then add the probability amplitudes of all the possibilities. This results in a superposition given by the state $|m_N \dots m_2 m_1\rangle$ after the transformation *Lambda* is performed. Assume that the system is lossless then the number of photons is preserved during the entire transformation.

Under the Heisenberg picture (quantum mechanical representation where time dependence is absorbed into the operator while keeping the basis fixed), the operators q_i and b_i evolve as:

$$q_i^\dagger \to b_i^\dagger = \sum_{k=1}^{N} \Lambda_{ik}^* q_k^\dagger = U^\dagger q_i^\dagger U \tag{1.66}$$

$$q_i \to b_i = \sum_{k=1}^{N} \Lambda_{ik} q_k = U^\dagger q_i U \tag{1.67}$$

Given that Λ is unitary, Eq.(1.66) can be rewritten:

$$Uq_i^\dagger U^\dagger = \sum_{k=1}^{N} \Lambda_{ki} q_k^\dagger \tag{1.68}$$

The number state when given an arbitrary input for the Nth mode can be generalized to:

$$|n_N \dots n_2 n_1\rangle = \frac{a_N^{\dagger n_N} \dots a_2^{\dagger n_2} a_1^{\dagger n_1}}{\sqrt{n_N! \dots n_2! n_1!}} |0 \dots 0\rangle \tag{1.69}$$

In order to find the exit state, the number state is operated on with U multiple times and keep in mind of the following property:

$$Uq_i^{\dagger 2} = Uq_i^\dagger I q_i^\dagger I = Uq_i^\dagger U^\dagger U q_i^\dagger U = (Uq_i^\dagger U^\dagger)^2 U \tag{1.70}$$

$$U|n_N \dots n_2 n_1\rangle = \frac{(Uq_N^\dagger U^\dagger)^{n_N} \dots (Uq_2^\dagger U^\dagger)^{n_2} (Uq_1^\dagger U^\dagger)^{n_1}}{\sqrt{n_N! \dots n_2! n_1!}} U|0 \dots 0\rangle \tag{1.71}$$

$$= \frac{\prod_{k=1}^{N} (\sum_{l=1}^{N} \Lambda_{lk} q_l^\dagger)^{n_k}}{\sqrt{n_N! \dots n_2! n_1!}} |0 \dots 0\rangle \tag{1.72}$$

1.3.5 Quantum Walks

Introduction

Much of the background in this section is attributed to Dr. Kempe on his explanation of the concept of Quantum Random Walks in the journal *Contemporary Physics* (Kempe, 2003).

A random walk is a stochoastic or random process that describes a path that consists of succession of random steps on a mathematical space. In the relevant application of Computational Chemistry, this could be the path traced by a molecule or an electron or a photon as it travels in a liquid or gas or around a molecule. Quantum walks are the quantum analogue of a classical random walk (Aharonov et al., 1993). One must be careful to use the phrase *quantum random walk* because

even though a measurement is random, the *evolution* of the state after the walk itself is not random but *unitary* compared to a classical random walk where the evolution of the walk is random based on a defined mathematical space (Fitzpatrick, 2017).

The main idea behind quantum random walks is to iterate the walk by repeating the succession of some unitary translation U and rotation $R(\theta)$ without the needed measurement M_z at intermediate time steps. Additionally, the position space of the particle must be discretized into a finite space such as a lattice or a graph. Quantum computers function with discrete registers where the Hilbert space is large but finite. A quantum computer should be able to simulate a quantum walk efficiently and use the simulation to solve computational problems which leads to uncovering efficient and fast algorithms. In principle any quantum algorithm can be simulated by a quantum walk. A multi-particle quantum walk (involving interacting many-body systems) may be used as an architecture for building a scalable quantum computer without the need for time-dependent control (Childs et al., 2013).

Before looking at the structure of quantum walks, let us visit Classical Discrete Random Walks, particularly those on a line with a particle jumping either left or right. For example, if we have a lattice with N nodes with each node having 6 vertices and the outcome of the particles moment is dependent on a dice roll described by a stochastic process $\{Z_n\}$. We can describe the probability of going to the right as p and to the left as $1-p$. We may describe each step by a Bernoulli-distributed random variable where the probability of finding the particle in position k after n steps and having an initial position $Z_0 = 0$ is given by the binomial distribution:

$$T_n = \sum_{k=1}^{n} Y_i = \frac{1}{2}(Z_n + n) \tag{1.73}$$

$$P(Z_n = k|Z_0 = 0) = \begin{cases} \binom{n}{\frac{1}{2}(k+n)} p^{\frac{1}{2}(k+n)} q^{\frac{1}{2}(n-k)}, & \frac{1}{2}(k+n) \in \mathbb{N} \cup \{0\}; \\ 0, \text{otherwise} \end{cases} \tag{1.74}$$

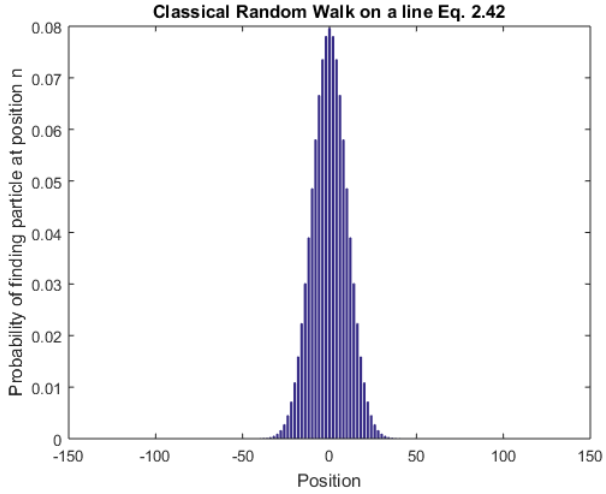

Figure 1·3: MATLAB Plot of Eq. 1.74 for $n = 100, p = \frac{1}{2}$. The probability of finding the particile at position $k = 0$ is equal 0.0795.

The structure of quantum walks can be built up and understood from the example of a *discrete time quantum walk* (DTQW). This sort of DTQW which will be shown is of a coined DTQW which consists of the following components - a walker, a coin, and a set of observables (Venegas-Andraca, 2012). The walker will consist of a infinite dimensional space Hilbert space $\mathcal{H}_p$ with a quantum system. Position states $|n\rangle$ will be in this Hilbert space with $|i\rangle_p$ basis states spanning the space as well. The walker will be initialized at the origin: $|n\rangle_{initial} = |0\rangle_p$. The coin will be a quantum system within a two-dimensional hilbert space $\mathcal{H}_c$, and thus will take states of either $|0\rangle$ or $|1\rangle$. The state $|c\rangle \in \mathcal{H}_c$ with a generalized expression in the form of $|c\rangle = a\,|0\rangle_c + b\,|1\rangle_c$.

The total state of the quantum walk will reside in the total Hilbert Space: $\mathcal{H}_t = \mathcal{H}_p \otimes \mathcal{H}_c$. Next part of the process is to define an evolution operator to be applied to the coin state following by a conditional shift operator to the total quantum system.

The coin operator will put the coin state into a superposition and then randomness is introduced by performing an measurement on the system after the two evolution operators are applied several times. We define the coin operation $\hat{C}$, the *Hadamard Operator* to apply a unitary rotation on the coin basis:

$$\hat{H} = \frac{1}{\sqrt{2}}(|0\rangle_c \langle 0| + |0\rangle_c \langle 1| + |1\rangle_c \langle 0| - |1\rangle_c \langle 1|) \tag{1.75}$$

Next, the *conditional translation* is applied to a position state (walker) to go one step forwards or backwards depending on basis state of the accompanying coin state. An appropriate conditional shift operator has the form:

$$\hat{S} = |0\rangle_c \langle 0| \otimes \sum_i |i+1\rangle_p \langle i| + |1\rangle_c \langle 1| \otimes \sum_i |i-1\rangle_p \langle i| \tag{1.76}$$

The total unitary operation on the total Hilbert space $\mathcal{H}_t$ is given by:

$$\hat{U} = \hat{S} \cdot (\hat{C} \otimes \hat{\mathbf{1}}_p) \tag{1.77}$$

The discrete quantum walk after t steps is given by:

$$|\psi\rangle_t = (\hat{U})^t |\psi\rangle_{initial} \tag{1.78}$$

Now the last ingredient for the Quantum Walks is a set of Observables. Interference effects between the coin and the walker from several iterations of applying $\hat{U}$ as well as entanglement between the walker(s) and coin(s) provided an advantage over classical walks. A measurement must be made to know the outcome of the walk. The set of observables will be based on the basis states used to define the coin and the walker.

One may perform a measurement on the coin by using the following observable:

$$\hat{M}_c = \alpha_0 |0\rangle_c \langle 0| + \alpha_1 |1\rangle_c \langle 1| \tag{1.79}$$

Afterwards, a measurement has to be made on the position states of the walker by the following operator:

$$\hat{M}_p = \sum_i \alpha_i \left|i\right\rangle_p \left\langle i\right| \tag{1.80}$$

I present a python simulation of a coined discrete quantum walk with 100 iterations.

Quantum Walk Simulation Example

The following parameters are used for this example simulation:

The number of iterations $t_{step} = 100$.

Coin Operator of the following rotation matrix form with angle $\theta = \pi/4$:

$$\hat{C} = \begin{bmatrix} \cos\theta & \sin\theta \\ \sin\theta & -\cos\theta \end{bmatrix} \tag{1.81}$$

With the following initial wavefunction on 2D basis:

$$\left|\psi\right\rangle_{initial} = \frac{\left|0\right\rangle + i\left|1\right\rangle}{\sqrt{2}} \tag{1.82}$$

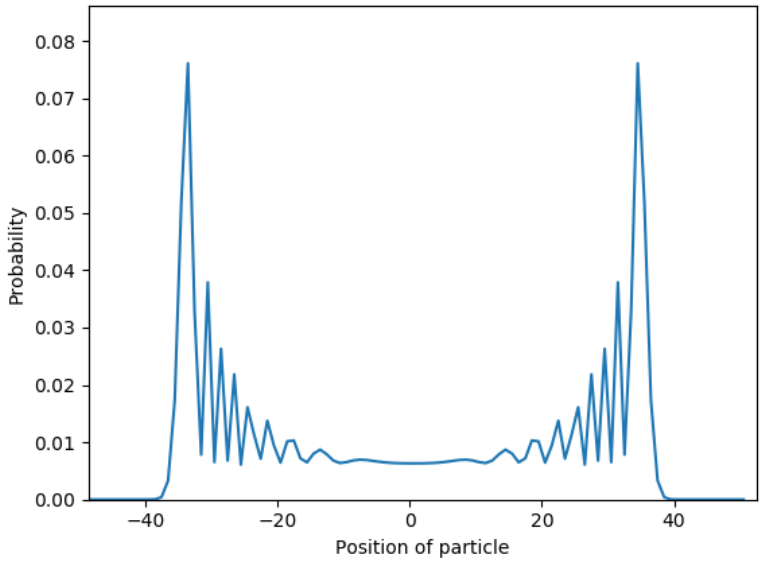

Figure 1·4: Probability distribution of 100 steps DTQW using the above defined coined and translational operators

Quantum Walks on a Graph & Scattering Theory

In the context of my thesis, the concept of quantum walks on a *graph* is necessary, particularly based on scattering theory as presented by Dr. Feldmann and Dr. Hillery (Feldman and Hillery, 2004). In this scenario, the walker is incident at a vertex or node of a graph with n edges. The particle possesses a reflection and transmission amplitude corresponding to the particle behavior at entering or exiting a particular vertex. The basis states for the particle correspond to the *momentum* on the edge. Therefore any operator acting in a graph with n edges will have dimensions $2n$.

Let O be the vertex at which all the edges be meet, with the opposite ends of the edges labeled with numbers 1 to n. Given any input state $|kO\rangle$ where k is an integer from 1 to n, the transition rule gives the amplitude to go to the output state $|Ok\rangle$ is given as r and the amplitude for any other output state is t. Evolution is unitary under the beam splitter conditions of the following amplitudes:

$$(n-1)|t|^2 + |r|^2 = 1 \tag{1.83}$$

$$(n-2)|t|^2 + r^*t + t^*r = 0 \tag{1.84}$$

This approach allows for not needing a Hilbert space for the coin states which reduces the dimensionality of a system.

1.4 Purpose of this Project

The purpose of this thesis is to demonstrate the utilization of simple quantum simulations to model the physical phenomena of a complex physical system such as a molecular system. The molecular system in my thesis to be investigated is that of Benzene (C_6H_6). If a molecular system like Benzene can be modeled through optical quantum simulations, then such simulations can be scaled up to more complicated or larger molecules. Utilizing Benzene as a testing ground will allow us to understand the accuracy, efficiency, and limits of proposed methods. The benzene molecule will be modeled optically through an arrangement of directionally unbiased multiports (three-port in the context of this thesis). Running quantum simulations will be highly beneficial to the medical and pharmaceutical industry for its potential for creating complex models of how the human body functions or modeling the processes governing chemical reactions leading to faster drug discovery for complex diseases such as cancer. Benzene (aromatic hydrocarbon, component of crude oil and gasoline, and produced across the U.S. in plastics, resins, etc.) is a cause of acute myeloid leukemia and other malignancies (McHale et al., 2012). Benzene is often used as a probe in identifying and characterizing binding pockets of proteins for structural design. Simulating the energy dynamics of benzene will allow researchers to learn more about the chemical processes governing benzene for designing better drugs or probes. If our proposed methods are successful then this will allow researchers to model other hydrocarbons or chemical systems such as Curcumin ($C_{21}H_{20}O_6$) which has anticancer benefits but hasn't been extensively studied and modeled yet (Ravindran et al., 2009).

Chapter 2

Motivation

2.1 Concept Development

Scientists & Engineers have studied the basic fundamentals governing atoms and electrons; however, a molecule contains too many interactions for modern day computers to fully calculate. As a result, drug development is very slow and expensive. To add on to this, the amount of transistor scaling is reaching a limit as Moore's Law slows down due to circuits approaching fundamental limits. Amdahl's law tells us that adding more processors can only get us so far as even parallelization has its speed limits. Lastly, supercomputers are very power hungry and as a result the more we scale up supercomputers the more exponentially power hungry these systems become. Quantum Computers could significantly extend the ability to simulate the structure and properties of molecules, including how chemicals, drugs, and hormones interact with the human body. Through large scale analytics and machine learning, quantum computing can give more information on gene expression and the origin of mutations which will be beneficial to clinical studies.

There is a variety of quantum computing architectures available such as trapped ions (Blatt, 2012), quantum annealing (Das and Chakrabarti, 2008) , superconducting qubits (Paraoanu, 2014) and in the context of my thesis-single photons (Broome et al., 2010). Available setups in the market and R&D involve very large scale setups along with the need of cooling down these systems down to near $0K$ temperatures which would not be as desirable long term. The utilization of photonic systems

would be a worthy competitor in quantum computing technology as they can perform in room temperature with simple optical components and have the potential to be scaled down to on-chip systems. One problem with these systems is that the photons do not interact as easily and this leads to a naturally decoherence-free system but complicates entanglement generation. Photons are not restricted to interactions with nearest neighbours due to their abiility to move freely in free space or in waveguides. In an on-chip system, free photon mobility gives arbitrary interconnections and allows simulations of complex and non-local many-body interactions (Aspuru-Guzik and Walther, 2012).

This leads us to the mobility of photons allowing us to simulate Quantum Walks through single-photon or multi-photon experiments. Multi-photon experiments provide novel affects in quantum walks. Loop-based architectures have been enabled up to 28 step discrete walks (Schreiber et al., 2010). Our system will essentially have photons going on a Quantum Walk around a 3 node closed system which one can generalize as a quantum walk around a N-node circle. Tuning the phase angles in our setup will allow for adjusting the eigenenergies and eigenstates to a close enough threshold that is comparable to the eigenenergies and eigenstates of the chosen simulated molecule which in our case is a Benzene molecule. Also, the concept of having quantum walks around a N-node circle allow for photon-photon interaction which is one of the current shortcomings in Optical Quantum Computing that needs to be overcome. Mixing time on the circle increases quadratically faster than a classical random walk (Bian et al., 2017).Success in performing these experiments and simulations will provide a testing ground to scale up our setup to other molecules and provide a framework for potential on-chip integration especially once one is able to keep entangled pairs of photons for a sufficient amount of time.

Chapter 3

System Description

3.1 Experiemental Abstraction

The following abstraction is what one should experiment when creating a full optical benzene model with our foundation. This abstraction also allows us to form the mathematical model that we will define later on. Note, that the abstraction does not include the inputs for the laser, measurement sites, optical circulators, any other necessary equipment. An optical schematic and laboratory picture of a single optical triport setup will be presented in the section following this one.

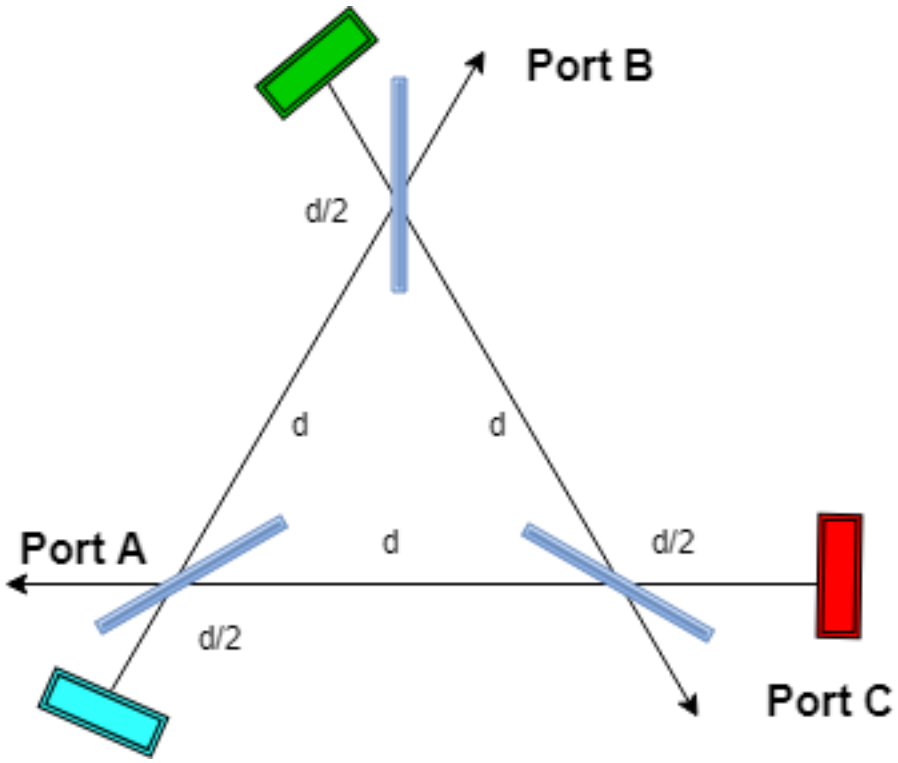

Figure 3·1: The Directionally-Unbiased Optical Three port. The thin blue rectangles represent the directionally-unbiased beam splitters. The colored rectangles represent the mirror units which contain a phase shifter and a mirror.

The optical multiport is in the arrangement of a triangular 3-port (as shown above) which consists of phase shifters, mirrors, and beam splitters at each of the three ports. The beam splitters in the multiport are directionally unbiased which means light going into a port can also have the option to exit out the same port. Since Benzene has 6 vertices of carbon, there will be 6 triports connected to one another. Two ports of the triport will connect to two ports of another triport to represent a double-bond connection and the remaining single port connections will represent a single-bond. The unbiased multiport is distinguished from regular beam splitters and multiports by their high levels of summetry and reversibility of the photon's movement through the system which make them more distinct from ther standard devices. Here in the

abstraction, the ports are an equivalent distance d apart. The labeled ports will allow us to describe a mathematical standard basis of vectors when constructing the Hamiltonian of the system. In the case of this thesis, I will choose B and C to be the two-ports to make the *double-bond* connection to the B and C port of an adjacent triport and port A to be used for representing the *single-bond* connection to the A port of the adjacent triport. Therefore, there will be three edges with double bonds and three edges with single bonds which will correspond to a single bond. The abstract construction of the optical benzene will be modeled mathematically for the construction of the Hamiltonian and its associated eigenvalues and eigenstates of the system.

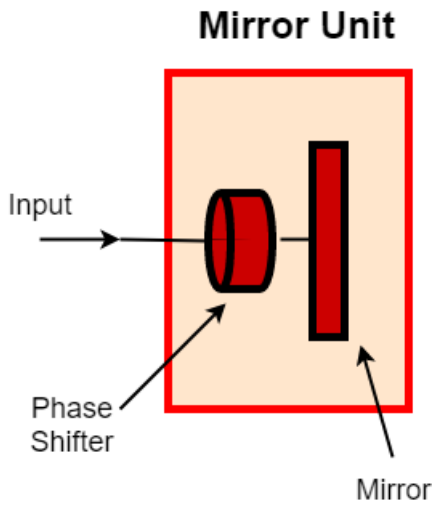

Figure 3·2: The Mirror Unit which consists of a phase shifter and a mirror. The distance between each beam splitter and the adjacent mirror is half the distance d between one beam splitter and the other. The phase shifter will be helpful in controlling the phase of the photons and interference of photon paths.

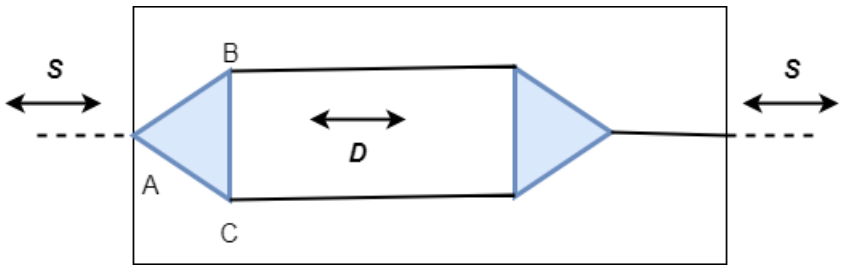

Figure 3·3: The Unit Cell of two directionally-unbiased triports connected to represent a double bond of a benzene system and the other end representing a single bond. Three of these unit cells will make up the optical benzene setup. S (single-bond state) and D (double-bond state) will later on be used to represent in bond states of the cell in our Hamiltonian model.

(a) Actual Benzene Molecule

(b) Optical Benzene System

Figure 3·4: Side by Side of a Benzene molecule (C_6H_6) with the abstraction of our Optical Benzene molecule. Photons injected into the optical system will undergo quantum random walks around the system analagous to the electron movement in the aromatic ring of a Benzene molecule

3.2 Laboratory Setup of Single Optical Triport

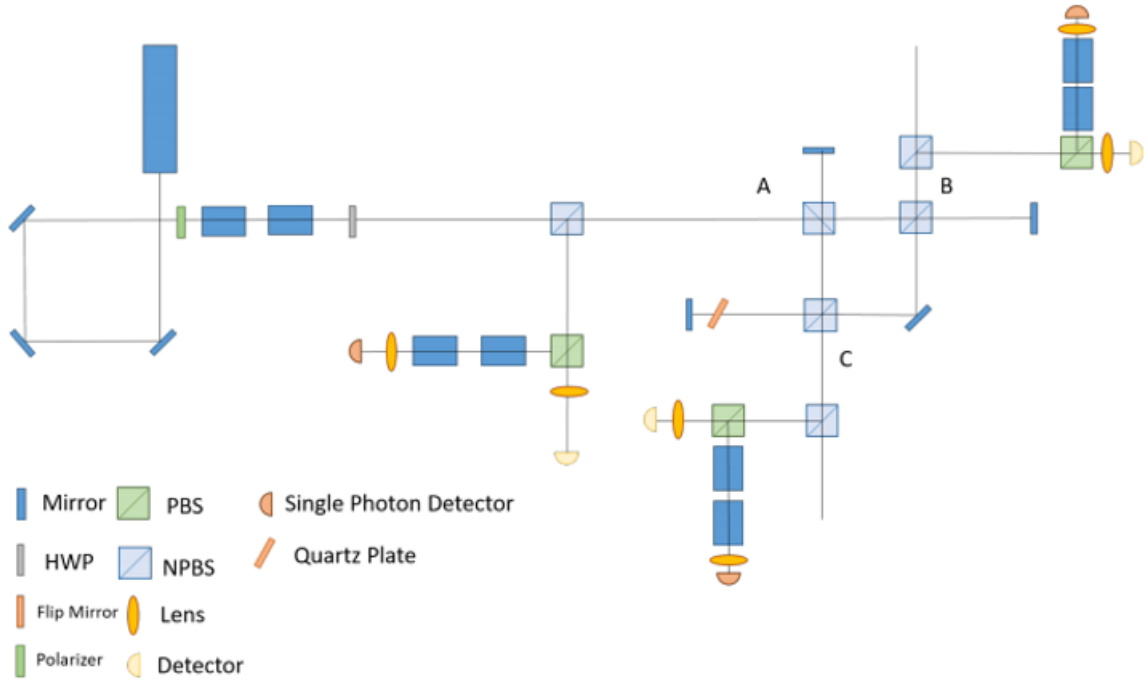

Figure 3·5: Optical Schematic of a Single Optical Triport

Our 633 nm laser delivers a stream of photons that bound around mirrors and into polarizing beam splitters which allow us to prepare the input states of the photons before they enter the field of three beam splitters which represent the three ports of the triport as shown in Fig. 4.1. The mirror units in this schematic only contain a mirror as the mirrors are laying on a translational stage which will act as the phase shifter in our setup. The beam will eventually lead out into a detector positioned a bit off in the setup. This setup seems more complicated than our abstracted setup due to practice problems arising such as attempting to allign a beam splitters at angles other than 45 or 90 degrees.

3.3 Software Implementation

Software implementation for the simulation and numerical analysis of the optical Benzene model is done on Python 3.6 with assistance with the QuTip Python Quantum Computing Toolbox.

Optical Benzene Numerical Analysis Class

1. Uses port phase angle ϕ as tunable parameter
2. Sets the amplitudes of the unitary matrix for a three-port device
3. Includes Pandas Options for readable matrix outputs
4. Constructs Hamiltonian from Unitary Matrix
5. Solves for Eigenvalues and Eigenvectors
6. Constructs Photon movement Projected out Hamiltonian and associated eigenvaleus and eigenvectors

Script for plotting Eigenspectrum and Eigenstates for Optical Benzene

1. Creates plots of the Eigenvalues (Eigenenergies) as a function of the phase angle ϕ for all Eigenvalues for either Hamiltonian
2. Creates plots of the probability amplitudes of the Eigenstates as a function of the state for a given eigenvalue at a given phase angle ϕ

Chapter 4

Optical Benzene Model

4.1 Basis Formulation

The Hamiltonian provides the energy dynamics and information of a quantum mechanical system. By solving the Time-Independent Schrodinger Equation:

$$H\left|\psi_n\right\rangle = E_n\left|\psi_n\right\rangle \tag{4.1}$$

one may arrive at the eigenvalues E_n which correspond to the energy levels of a molecular system and the eigenenergies have associated eigenvectors $|\psi_n\rangle$ which describe the associated state of the system i.e. position, momentum etc.

I define a basis for the multiport connected benzene system. The unit cells of the connected triports will be defined by the following 12×12 Hilbert space:

$$\mathcal{H} = |n\rangle \otimes |M\rangle \otimes |B\rangle \tag{4.2}$$

Where $n \in \{1, 2, 3\}$ represent the unit cell index corresponding to the 3 unit cells (6 triports) of the optical benzene, $m \in \{L, R\}$ represents the left and right moving states of a photon in the system, and $B \in \{S, D\}$ represent the single and double states of a photons position within a unit cell. Note that this system is cyclic with n mod 3.

4.2 States of the System

4.2.1 Triport Representation

The Ports A, B, C of the 3-port optical multiport form a 3-dimensional standard basis:

$$|A\rangle = \begin{pmatrix} 1 \\ 0 \\ 0 \end{pmatrix}, |B\rangle = \begin{pmatrix} 0 \\ 1 \\ 0 \end{pmatrix}, |C\rangle = \begin{pmatrix} 0 \\ 0 \\ 1 \end{pmatrix} \tag{4.3}$$

4.2.2 Unit Cell Representation

Based on Fig 3.3 and the the Hilbert Space of this system, the single bond state S is taken to be port A of a optical triport and the double bond state D is taken to be port B and C of a optical triport. Using Eq. 4.3 one may define the double bond states of the B space as the following:

$$|S\rangle = |A\rangle = \begin{pmatrix} 1 \\ 0 \\ 0 \end{pmatrix} \tag{4.4}$$

$$|D\rangle = \frac{1}{\sqrt{2}}(|B\rangle + |C\rangle) = \frac{1}{\sqrt{2}} \begin{pmatrix} 0 \\ 1 \\ 1 \end{pmatrix} \tag{4.5}$$

One may also reduce the representation of the bond states to a 2-dimensional standard basis which will be used for a specific case later on:

$$|S\rangle = \begin{pmatrix} 1 \\ 0 \end{pmatrix}, |D\rangle = \begin{pmatrix} 0 \\ 1 \end{pmatrix} \tag{4.6}$$

4.3 Directionally-Unbiased Optical Three-Ports

It is important to derive the photon dynamics within a single directionally unbiased optical three-port device In order to this, the unitary matrix that describe the transitions from one port to another port in a three-port must be derived. (Simon et al., 2016).

Assume that a photon into Port A. Due to the reflection symmetry in the input direction, the exit amplitudes for the other two ports should be equal. So given an input state $|\psi_{in}\rangle = |A\rangle$ then the output is of the form:

$$|\psi_{out}\rangle = a\,|A\rangle + b(|B\rangle + |C\rangle) \tag{4.7}$$

With complex amplitudes a and b. Repeating the argument for inputs B and C , the transition matrix V is of the form :

$$V = \begin{pmatrix} a & b & b \\ b & a & b \\ b & b & a \end{pmatrix} \tag{4.8}$$

The matrix is unitary, therefore $V \cdot V^{\dagger} = I$, the diagonal and off-diagonal entries must satisfy the normalization constraints:

$$|a|^2 + 2|b|^2 = 1, 2Re(ab^*) + |b|^2 = 0 \tag{4.9}$$

Define the following:

$$a = \alpha e^{i\phi_a}, b = \beta e^{i\phi_b} \tag{4.10}$$

$$\phi = \phi_b - \phi_a \tag{4.11}$$

Solving for Eqn (8) and (9) gives:

$$\alpha = \sqrt{\frac{1}{1 + 8\cos^2\phi}} \tag{4.12}$$

$$\beta = -2\sqrt{\frac{\cos^2\phi}{1 + 8\cos^2\phi}} \tag{4.13}$$

Putting it all together V becomes of the following form:

$$V = \frac{e^{i\phi_a}}{\sqrt{1 + 8\cos^2\phi}} \begin{pmatrix} 1 & -2e^{-i\phi}\cos\phi & -2e^{-i\phi}\cos\phi \\ -2e^{-i\phi}\cos\phi & 1 & -2e^{-i\phi}\cos\phi \\ -2e^{-i\phi}\cos\phi & -2e^{-i\phi}\cos\phi & 1 \end{pmatrix} \tag{4.14}$$

The special case of $\phi = 0$ gives

$$V(\phi_a) = \frac{1}{3} e^{i\phi_a} \begin{pmatrix} 1 & -2 & -2 \\ -2 & 1 & -2 \\ -2 & -2 & 1 \end{pmatrix} \tag{4.15}$$

More generally, for the context of this research, all 3 ports are set equal to one another and set as a single tunable paramter ϕ, provides a unitary matrix U of the following form:

$$\phi = \phi_A = \phi_B = \phi_C \tag{4.16}$$

$$U = \frac{e^{i\phi}}{2 + ie^{i\phi}} \begin{pmatrix} 1 & ie^{-i\phi} - 1 & ie^{-i\phi} - 1 \\ ie^{-i\phi} - 1 & 1 & ie^{-i\phi} - 1 \\ ie^{-i\phi} - 1 & ie^{-i\phi} - 1 & 1 \end{pmatrix} \tag{4.17}$$

4.4 The Full General Model

4.4.1 System Interactions

Given our full 12×12 Hilbert Space and the Unitary matrix for a single three-port, we now derive the transitions for a photon within the optical three-port connected benzene model.

The transitions within the optical benzene system described by the three state spaces– unit cell index (cyclic mod 3, $n-1, n, n+1$), right/left moving (R/L) and bond sites (S/D) are given as the following:

1. $SR \to DR, n \to n+1, n+1 \to n-1, n-1 \to n$
2. $DR \to SR, n, n+1, n-1$ fixed
3. $SR \to SL, n, n+1, n-1$ fixed
4. $DR \to DL, n, n+1, n-1$ fixed
5. $SL \to DL, n, n+1, n-1$ fixed

6. $DL \to SL, n \to n-1, n+1 \to n, n-1 \to n+1$

7. $SL \to SR, n, n+1, n-1$ fixed

8. $DL \to DR, n, n+1, n-1$ fixed

4.4.2 Transition Amplitudes

First, for simplicity we define new variables for the amplitude value and unitary matrix scaling term in Eq. (4.17):

$$\beta = \frac{e^{i\phi}}{2 + ie^{i\phi}} \tag{4.18}$$

$$\rho = ie^{-i\phi} - 1 \tag{4.19}$$

Transition Amplitudes between the bond sites in terms of the bond states are as follows (β appears in all as it is a factor outside the unitary matrix):

$$S \Longleftrightarrow S \to \langle A|A\rangle = \beta \tag{4.20}$$

$$S \Longleftrightarrow D \to \frac{1}{\sqrt{2}} \langle A|B + C\rangle = \frac{2}{\sqrt{2}}\rho\beta = \sqrt{2}\rho\beta \tag{4.21}$$

$$D \Longleftrightarrow D \to \frac{1}{2} \langle B + C|B + C\rangle = \frac{1}{2}(\langle B|B\rangle + \langle C|C\rangle + 2\,\mathrm{Re}\,\langle B|C\rangle) = \beta(1+\rho) \tag{4.22}$$

4.4.3 Full Unitary Matrix Formulation

Given these amplitudes and transition information, we can now construct the full 12 by 12 Unitary matrix for a state $|B, M, n\rangle$ where $B \in \{S, D\}$ (bond states) , $M \in \{L, R\}$ (motion of photon - left or right), $n \in \{1, 2, 3\}$ (unit cell index). Due to cyclical behaviour one can create a 3 by 3 block circulant matrix where the block matrices are 4 by 4:

$$\hat{U} = \beta \begin{pmatrix} \Lambda_1 & \Lambda_2 & \Lambda_3 \\ \Lambda_3 & \Lambda_1 & \Lambda_2 \\ \Lambda_2 & \Lambda_3 & \Lambda_1 \end{pmatrix} \tag{4.23}$$

Where $\Lambda_1, \Lambda_2, \Lambda_3$ represent the following matrix blocks:

$$\Lambda_1 = \begin{array}{c} \begin{matrix} |SLn\rangle & |SRn\rangle & |DLn\rangle & |DRn\rangle \end{matrix} \\ \begin{pmatrix} 0 & 1 & 0 & 0 \\ 1 & 0 & 0 & \sqrt{2}\rho \\ \sqrt{2}\rho & 0 & 0 & 1+\rho \\ 0 & 0 & 1+\rho & 0 \end{pmatrix} \end{array} \begin{matrix} |SLn\rangle \\ |SRn\rangle \\ |DLn\rangle \\ |DRn\rangle \end{matrix} \tag{4.24}$$

$$\Lambda_2 = \begin{array}{c} \begin{matrix} |SLn\rangle & |SRn\rangle & |DLn\rangle & |DRn\rangle \end{matrix} \\ \begin{pmatrix} 0 & 0 & \sqrt{2}\rho & 0 \\ 0 & 0 & 0 & 0 \\ 0 & 0 & 0 & 0 \\ 0 & 0 & 0 & 0 \end{pmatrix} \end{array} \begin{matrix} |SLn-1\rangle \\ |SRn-1\rangle \\ |DLn-1\rangle \\ |DRn-1\rangle \end{matrix} \tag{4.25}$$

$$\Lambda_3 = \begin{array}{c} \begin{matrix} |SLn\rangle & |SRn\rangle & |DLn\rangle & |DRn\rangle \end{matrix} \\ \begin{pmatrix} 0 & 0 & 0 & 0 \\ 0 & 0 & 0 & 0 \\ 0 & 0 & 0 & 0 \\ 0 & \sqrt{2}\rho & 0 & 0 \end{pmatrix} \end{array} \begin{matrix} |SLn+1\rangle \\ |SRn+1\rangle \\ |DLn+1\rangle \\ |DRn+1\rangle \end{matrix} \tag{4.26}$$

4.4.4 Full Hamiltonian Model

In order to obtain the Hamiltonian from the Unitary Matrix, we solve the Time-Dependent Schrodinger Equation:

$$\frac{d\left|\psi\right\rangle_{BMn}}{dt} = -i\frac{\hat{H(t)}}{\hbar} \tag{4.27}$$

The Unitary Operator $\hat{U}$ is a wave equation solution and describes the time-evolution of the eigenstates expressed as:

$$\hat{U} = e^{-iHT/\hbar} \tag{4.28}$$

Where T is time and $\hbar$ is the reduced Planck's constant. For simplicity we will set $T = \hbar = 1$ leading to:

$$U = e^{-iH} \tag{4.29}$$

Given that U and H are both matrices, we take the matrix logarithm operation on both sides (can be computed through various numerical approximations and method, see Appendix A.2 for more information) and this provides the Hamiltonian as the following:

$$H = i\ln U \tag{4.30}$$

One can verify analytically that our Unitary matrix U holds the Unitary Condition:

$$UU^{\dagger} = I \tag{4.31}$$

Afterwards, one can verify numerically that the Hamiltonian holds the Hermiticity Condition:

$$H = H^{\dagger} \tag{4.32}$$

4.5 Reduced General Model without Direction of Movement

Given the 6 Carbon atom nature of a Benzene molecule, there is going to be a set of 6 energy levels and energy states and thus we'd like to also have a Hamiltonian model that is reduced down to that size. We do this by projecting out the M vector space that describes the movement of a photon in the system as either leftmoving L or rightmoving R.

4.5.1 Projection Operator

In order to reduce our Hilbert Space, we define a projection operator that when acted upon the full 12 by 12 vector space, gets reduced down to a 6 by 6 space via the Hamiltonian being projected onto the diagonal subspace of the left-and right-moving modes.

$$\mathcal{H} = |n\rangle \otimes |M\rangle \otimes |D\rangle \rightarrow \mathcal{H}' = |n\rangle \otimes |B\rangle \tag{4.33}$$

$$\hat{P} = \sum_{Bond\&PositionSubspace} |m\rangle \langle m| \tag{4.34}$$

Given a state of the form $|B, M, n\rangle$ then the Projection operator is a superposition of left and right moving states that multiply across the Hamiltonian to form the matrix elements of the reduced Hamiltonian:

$$P = \frac{1}{\sqrt{2}}(|B, L, n\rangle \langle B, n, L| + |B, R, n\rangle \langle B, R, n|) \tag{4.35}$$

4.5.2 Reduced Hamiltonian Model

Using the Projection Operator above, one can apply it to our full Hamiltonian matrix by multiplying H on the left and right side with the hermitian conjugate of the projection operator and the projection operator respectively to obtain the reduced Hamiltonain H':

$$H' = P^{\dagger} H P \tag{4.36}$$

Chapter 5

Eigendecomposition of the System

5.1 Eigenvalues of Full Hamiltonian

In order to obtain the eigenenergies (eigenvalues) of the Hamiltonian, we solve the eigenvalue/eigenvector problem that arises from the Time-Independent Schrodinger Equation:

$$\hat{H}(\phi)\,|B, M, n\rangle = E_i(\phi)\,|B, M, n\rangle \tag{5.1}$$

Where $i = 1, 2, \ldots, 12$ and ϕ is the phase angle parameter for the multiports.
The eigenvalues arise from the following expression where one must solve for E_i:

$$\det(H - E_i I) = 0 \tag{5.2}$$

5.2 Eigenstates of Full Hamiltonian

Using the derived eigenvalues, one may solve the associated eigenstates (eigenvectors) of the Hamiltonian by plugging in the individual eigenvalues into Eq. (5.1) and solving for the values of the eigenvector by inspection or via Gaussian Elimination:

$$(H - E_i I)\,|\psi\rangle^{(i)}_{BMn} = 0 \tag{5.3}$$

Eigenstates must be normalized after being obtained:

$$|\,|\psi\rangle\,|^2 = 1 \tag{5.4}$$

5.3 Eigenanalysis for $\phi = \pi/2$

In a series of a few test cases of ϕ phase angles, we start with eigenanalysis for $\pi/2$ which produces some interesting results of the system collapsing to two 6-fold degenerate energy levels (full Eigenspectrum plot shown later in this thesis)

5.3.1 Parameter Values

Plugging in our phase angle of $\pi/2$ into our parameter values β, ρ that denote the transition amplitudes:

$$\beta(\pi/2) = \frac{e^{i\pi/2}}{2 + ie^{i\pi/2}} = i \tag{5.5}$$

$$\rho(\pi/2) = ie^{-i\pi/2} - 1 = 0 \tag{5.6}$$

5.3.2 Matrix Block Values

Given that the submatrices Λ_2, Λ_3 only contain one value which is $\sqrt{2}\rho$ and $\rho(\pi/2)$ is 0 , these submatrices become 0-matrix blocks leaving the Λ_1 submatrix as follows:

$$\Lambda_1(\pi/2) = \begin{pmatrix} 0 & 1 & 0 & 0 \\ 1 & 0 & 0 & 0 \\ 0 & 0 & 0 & 1 \\ 0 & 0 & 1 & 0 \end{pmatrix}, \Lambda_2 = \Lambda_3 = 0 \tag{5.7}$$

Given that other blocks are 0, one can exploit the symmetry of the matrix and find the eigenvalues of the Λ_1 block and extend it two more times.

It is evident that Λ_1 can be diagonalized and thus there exists a matrix S such that:

$$D = S\Lambda_1 S^{-1} \tag{5.8}$$

Where D is diagonalized matrix of Λ_1, this is found to be:

$$D = \begin{pmatrix} -1 & 0 & 0 & 0 \\ 0 & -1 & 0 & 0 \\ 0 & 0 & 1 & 0 \\ 0 & 0 & 0 & 1 \end{pmatrix} \tag{5.9}$$

5.3.3 Eigenvalues

If a matrix is diagonal, then the elements D_{ii} along the main diagonal are the eigenvalues of the matrix:

$$E^{U(\pi/2)}_{1,2,3,4,5,6} = -i = e^{-i\pi/2} \tag{5.10}$$

$$E^{U(\pi/2)}_{7,8,9,10,11,12} = i = e^{i\pi/2} \tag{5.11}$$

Now we take the natural log of each of the eigenvalues to produce the eigenvalues of the Hamiltonian:

$$E^{H(\pi/2)}_{1,2,3,4,5,6} = -\pi/2 \tag{5.12}$$

$$E^{H(\pi/2)}_{7,8,9,10,11,12} = \pi/2 \tag{5.13}$$

5.3.4 Eigenstates

The pair of 6-fold degeneracies at $\pm\pi/2$ produce eigenstates that show the photon is in a superposition of left or right moving within a bond site and unit cell position along the entire system which gives rises to non-stationary states.

This is evident from the Unitary Transformation showing only transitions between Left and Right Modes within a fixed unitcell and bond site.

Eigenvalue E	Eigenstate $\lvert B, M, n\rangle$
$-\pi/2$	$\frac{1}{\sqrt{2}}\Big[(1,1,0,0,\ldots,0)^T, (0,0,1,1,\ldots,0)^T,$ $(0,0,0,0,1,1,\ldots,0)^T, (0,0,0,0,0,0,1,1,\ldots,0)^T$ $(0,0,0,0,0,0,0,0,1,1,\ldots,0)^T, (0,\ldots,1,1)^T\Big]$
$\pi/2$	$\frac{1}{\sqrt{2}}\Big[(0,0,1,-1,\ldots,0)^T, (0,0,0,0,0,0,1,-1,\ldots,0)^T$ $(1,-1,\ldots,0)^T, (0,\ldots,1,-1,0,0)^T$ $(0,0,0,0,1,-1,\ldots,0)^T, (0,\ldots,1,-1)^T\Big]$

Table 5.1: Corresponding Eigenstates to the Eigenvalues for $H(\pi/2)$

5.3.5 Qualitative Description

For $E = -\pi/2$, each eigenstate is a steady state with the average photon reflecting from left to right within a fixed unit cell and fixed bond site.

For $E = \pi/2$, each eigenstate is a steady state with the average photon reflecting right to left within a fixed unit cell and fixed bond site.

5.4 Eigenanalysis for $\phi = 3\pi/2$

Now we traverse to the other side of the phase plane and look at $\phi = 3\pi/2$ which produces a more "opposite" effect than that of $\phi = \pi/2$. The system produces a set of six 2-fold degenerate energy levels.

5.4.1 Parameter Values

Pluggin in $\phi = 3\pi/2$ we get:

$$\beta(3\pi/2) = -\frac{i}{3} \tag{5.14}$$

$$\rho(3\pi/2) = -2 \tag{5.15}$$

5.4.2 Matrix Block Values

Plugging in the values above into the matrix blocks of the Unitary Matrix, we get the following:

$$\Lambda_1(3\pi/2) = \begin{pmatrix} 0 & 1 & 0 & 0 \\ 1 & 0 & 0 & -2\sqrt{2} \\ -2\sqrt{2} & 0 & 0 & -1 \\ 0 & 0 & -1 & 0 \end{pmatrix} \tag{5.16}$$

$$\Lambda_2(3\pi/2) = \begin{pmatrix} 0 & 0 & -2\sqrt{2} & 0 \\ 0 & 0 & 0 & 0 \\ 0 & 0 & 0 & 0 \\ 0 & 0 & 0 & 0 \end{pmatrix}, \Lambda_3(3\pi/2) = \begin{pmatrix} 0 & 0 & 0 & 0 \\ 0 & 0 & 0 & 0 \\ 0 & 0 & 0 & 0 \\ 0 & -2\sqrt{2} & 0 & 0 \end{pmatrix} \tag{5.17}$$

Due to the size and complexity of the matrix we define the Unitary Matrix as a sum of Kronecker Products in terms of some matrix P:

$$P = \begin{pmatrix} 0 & 1 & 0 \\ 0 & 0 & 1 \\ 1 & 0 & 0 \end{pmatrix} \tag{5.18}$$

$$3iU = I \otimes \Lambda_1 + P \otimes \Lambda_2 + P^2 \otimes \Lambda_3 \tag{5.19}$$

5.4.3 Eigenvalues

It is evident that Λ_2 and Λ_3 commute and are both nilpotent matrices ($N^k = 0$ for some square matrix N and integer k). his infers that $P \otimes \Lambda_2$ and $P^2 \otimes \Lambda_3$ are commuting nilpotent matrices. This follows that $P \otimes \Lambda_2 + P^2 \otimes \Lambda_3$ is a nilpotent matrix and by inspection the eigengvalue is 0 . It satisfies $(P \otimes \Lambda_2 + P^2 \otimes \Lambda_3)^2 = 0$. We require an invertible matrix S (columns are eigenvectors) to diagonalize Λ_1 such that we produce a diagonal matrix D:

$$D = S^{-1}\Lambda_1 S \tag{5.20}$$

The eigenvalues of Λ_1 are 4 distinct and complex valued roots of the characteristic polynomial:

$$p(x) = x^4 - 2x^2 + 9 \tag{5.21}$$

Let $V = 3iU$ for simplicity

$$(I \otimes S)^{-1} V (I \otimes S) = \begin{pmatrix} S\Lambda_1 S^{-1} & S\Lambda_2 S^{-1} & S\Lambda_3 S^{-1} \\ S\Lambda_3 S^{-1} & S\Lambda_1 S^{-1} & S\Lambda_2 S^{-1} \\ S\Lambda_2 S^{-1} & S\Lambda_3 S^{-1} & S\Lambda_1 S^{-1} \end{pmatrix} \tag{5.22}$$

$$= \begin{pmatrix} D & M_2 & M_3 \\ M_3 & D & M_2 \\ M_2 & M_3 & D \end{pmatrix} \tag{5.23}$$

$$= I \otimes D + P \otimes M_2 + P^2 \otimes M_3 \tag{5.24}$$

Solve the characteristic polynomial $p(x) = x^4 - 2x^2 + 9$

Let $w = x^2, w^2 = x^4$ and solve the substituted polynomial:

$$w^2 - 2w + 9 = 0 \tag{5.25}$$

$$w = 1 \pm 2\sqrt{2}i \tag{5.26}$$

$$x^2 = 1 \pm 2\sqrt{2}i \tag{5.27}$$

Let $x = u + iv$

$$(u + iv)^2 = 1 \pm 2\sqrt{2}i \tag{5.28}$$

$$u^2 - v^2 + 2iuv = 1 \pm 2\sqrt{2}i \tag{5.29}$$

$$\begin{pmatrix} u^2 - v^2 = 1 \\ 2uv = \pm\sqrt{2} \end{pmatrix} \rightarrow v = \pm 1, u = \pm\sqrt{2} \tag{5.30}$$

Therefore the roots of the characteristic polynomiam $p(x)$ for Λ_1 are:

$$x = \sqrt{2} + i, -\sqrt{2} - i, -\sqrt{2} + i, \sqrt{2} - i \tag{5.31}$$

With the following eigenvector space:

$$\vec{v} = \left\{ \begin{pmatrix} i \\ -1 + \sqrt{2}i \\ -i - \sqrt{2} \\ 1 \end{pmatrix}, \begin{pmatrix} i \\ 1 - \sqrt{2}i \\ i + \sqrt{2} \\ 1 \end{pmatrix} \begin{pmatrix} -i \\ 1 + \sqrt{2}i \\ -i + \sqrt{2} \\ 1 \end{pmatrix} \begin{pmatrix} -i \\ -1 - \sqrt{2}i \\ i - \sqrt{2} \\ 1 \end{pmatrix} \right\} \tag{5.32}$$

The eigenspace above makes up the matrix S and the diagonal matrix D is given by the 4 roots of the characteristic polynomial.

$$S = \begin{pmatrix} -i & -i & i & i \\ 1 + \sqrt{2}i & -1 - \sqrt{2}i & 1 - \sqrt{2}i & -1 + \sqrt{2}i \\ \sqrt{2} - i & -\sqrt{2} + i & \sqrt{2} + i & -\sqrt{2} - i \\ 1 & 1 & 1 & 1 \end{pmatrix} \tag{5.33}$$

$$D = \begin{pmatrix} -\sqrt{2}+i & 0 & 0 & 0 \\ 0 & \sqrt{2}-i & 0 & 0 \\ 0 & 0 & -\sqrt{2}-i & 0 \\ 0 & 0 & 0 & \sqrt{2}+i \end{pmatrix} \tag{5.34}$$

Since Λ_2 and Λ_3 are non-diagonizable , we find a Jordan Normal form them There exists a matrix M_2 and M_3 such that $\Lambda_2 = SM_2S^{-1}$ and $\Lambda_3 = SM_3S^{-1}$

$$\det(\Lambda_2 - xI) = \det\left(\begin{pmatrix} 0 & -x & -2\sqrt{2} & 0 \\ -x & 0 & 0 & 0 \\ 0 & 0 & -x & 0 \\ 0 & 0 & 0 & -x \end{pmatrix}\right) = \det\begin{pmatrix} A & B \\ C & D \end{pmatrix} \tag{5.35}$$

Since C and D commute:

$$\det(\Lambda_2 - xI) = -\det(AD - BC) = -\det\begin{pmatrix} 0 & x^2 \\ x^2 & 0 \end{pmatrix} = x^4 = 0 \tag{5.36}$$

Therefore there is one eigenvalue with a value of 0 with multiplicity 4

Via gaussian elimination one can find the matrix S and corresponding S^{-1} to be

$$S = \begin{pmatrix} 0 & 0 & 1 & 0 \\ 0 & 1 & 0 & 0 \\ 0 & 0 & 0 & -\frac{1}{2\sqrt{2}} \\ 1 & 0 & 0 & 0 \end{pmatrix} \tag{5.37}$$

$$S^{-1} = \begin{pmatrix} 0 & 0 & 0 & 1 \\ 0 & 1 & 0 & 0 \\ 1 & 0 & 0 & 0 \\ 0 & 0 & -2\sqrt{2} & 0 \end{pmatrix} \tag{5.38}$$

$$M_2 = S\Lambda_2 S^{-1} = \begin{pmatrix} 0 & 0 & 0 & 0 \\ 0 & 0 & 0 & 0 \\ 0 & 0 & 1 & 0 \\ 0 & 0 & 0 & 0 \end{pmatrix} \tag{5.39}$$

Similarly one can do the same for Λ_3:

$$S = \begin{pmatrix} 0 & 0 & 0 & 1 \\ 0 & -\frac{1}{2\sqrt{2}} & 0 & 0 \\ 0 & 0 & 1 & 0 \\ 1 & 0 & 0 & 0 \end{pmatrix}, S^{-1} = \begin{pmatrix} 0 & 0 & 0 & 1 \\ 0 & -2\sqrt{2} & 0 & 0 \\ 0 & 0 & 1 & 0 \\ 1 & 0 & 0 & 0 \end{pmatrix} \tag{5.40}$$

$$M_3 = S\Lambda_3 S^{-1} = \begin{pmatrix} 0 & 1 & 0 & 0 \\ 0 & 0 & 0 & 0 \\ 0 & 0 & 0 & 0 \\ 0 & 0 & 0 & 0 \end{pmatrix} \tag{5.41}$$

Putting it all together, to reduce the breadth of work one may numerically computing the resultant matrix and find the following eigenvalues for $U(3\pi/2)$:

$$E_{1,2}^{U(3\pi/2)} = 1.733 + 2.45i, E_{3,4}^{U(3\pi/2)} = 1.733 - 2.45i \tag{5.42}$$

$$E_{5,6}^{U(3\pi/2)} = -3.00148, E_{7,8}^{U(3\pi/2)} = 3.00148 \tag{5.43}$$

$$E_{9,10}^{U(3\pi/2)} = -1.733 - 2.45i, E_{11,12}^{U(3\pi/2)} = -1.733 + 2.45i \tag{5.44}$$

Taking $E_i^H = i \ln E_i^U$ we get:

$$E_{1,2}^{H(3\pi/2)} = 0.616, E_{3,4}^{H(3\pi/2)} = 2.53 \tag{5.45}$$

$$E_{5,6}^{U(3\pi/2)} = -\pi/2, E_{7,8}^{U(3\pi/2)} = \pi/2 \tag{5.46}$$

$$E_{9,10}^{U(3\pi/2)} = -2.53, E_{11,12}^{U(3\pi/2)} = -0.616 \tag{5.47}$$

5.4.4 Eigenstates

The six 2-fold degeneracies produce four eigenstates with probability amplitude values that are periodic and eight eigenstates that have a mixture of probability amplitude values. The probability amplitude spectrum of the periodic behaviour eigenstates are shown below.

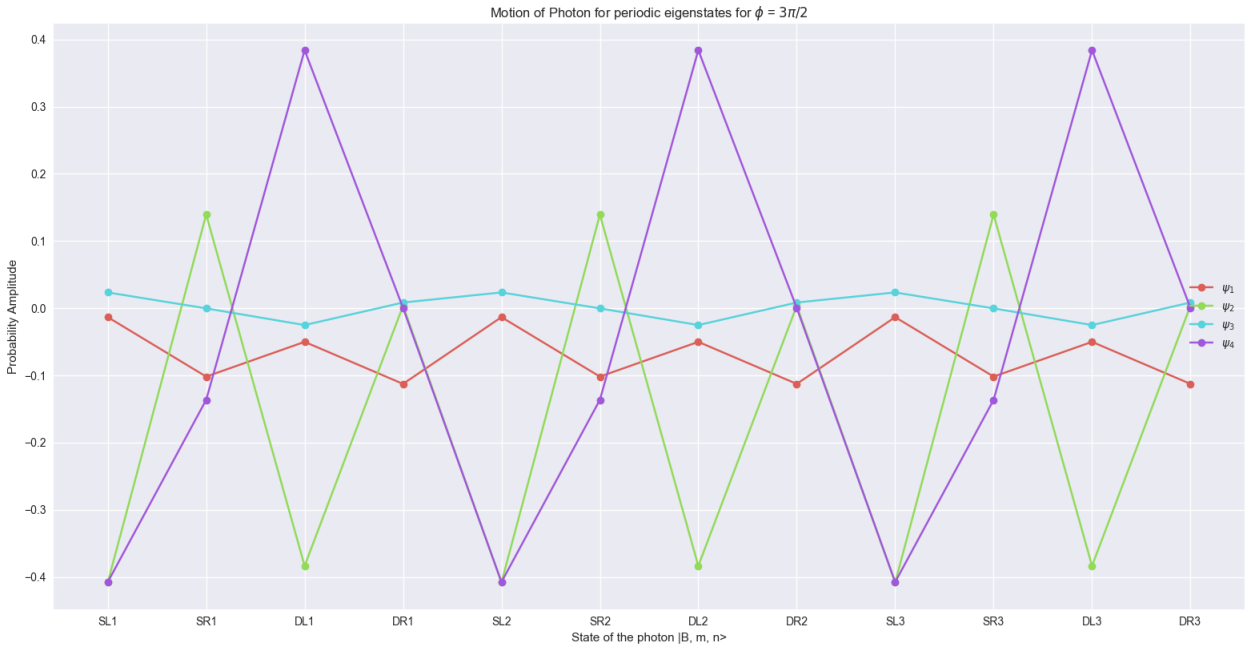

Figure 5·1: Probability Amplitudes as a function of the state $|B, M, n\rangle$ of the periodic behaviour Eigenstates for the associated Eigenvalues for the full Hamiltonian evaluated with a multiport phase angle of $3\pi/2$

ψ_1(red) and ψ_2(green) belong to the degenerate pair of energy $-\pi/2$ and ψ_3(blue) and ψ_4(purple) belong to the degenerate pair of energy $\pi/2$.

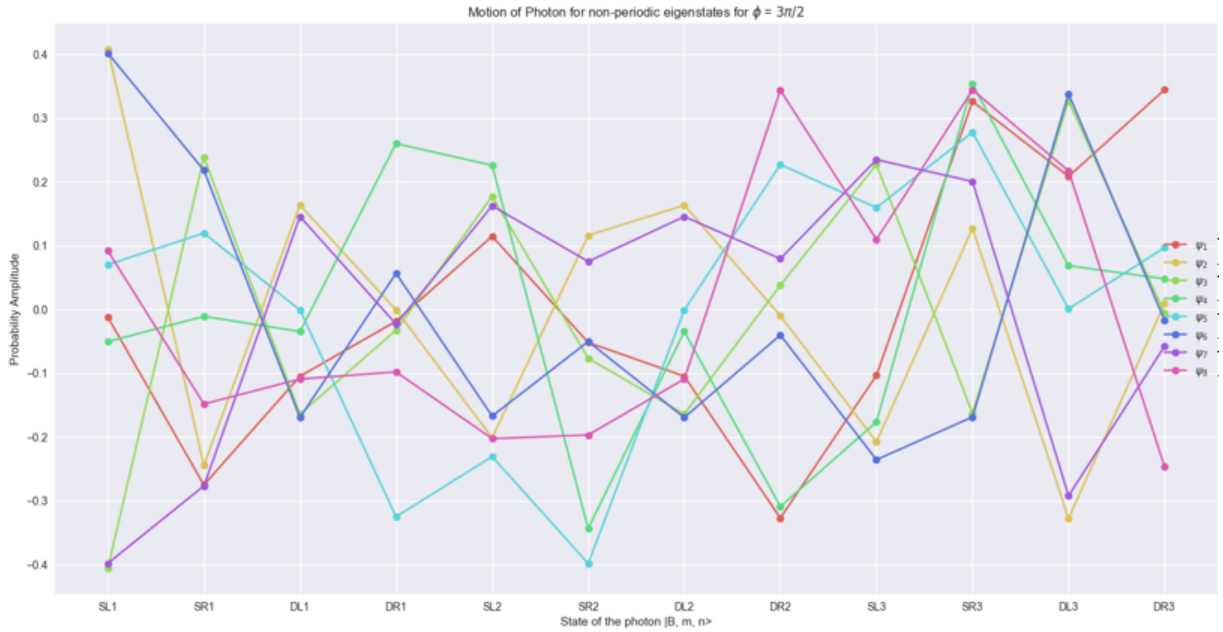

Figure 5·2: Probability Amplitudes as a function of the state $|B, M, n\rangle$ of the mixed behaviour Eigenstates for the associated Eigenvalues for a Hamiltonian evaluated with a multiport phase angle of $3\pi/2$

5.4.5 Qualitative Description

The four periodic behaving eigenstates exhibit photon transitions between unitcells while maintaining the transition on a fixed bond site and direction of movement. Given the mixed and random-esque nature of the other eight eigenstates, one cannot deduce any particular pattern of photon movement at those other energy levels.

5.5 Eigenspectrum for Full Hamiltonian

Numerically we find the full Eigenvalue (Eigenenergy) Spectrum of the Hamiltonian matrix:

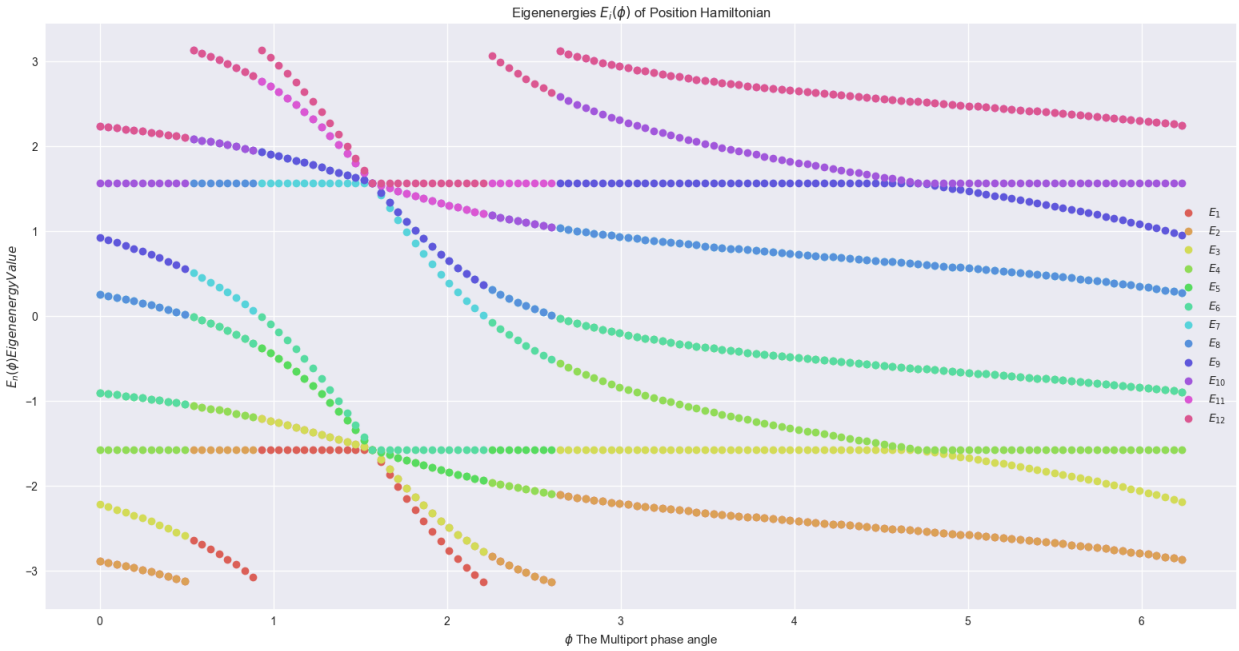

Figure 5·3: Eigenvalue/Eigenenergy $E_i(\phi)$ spectrum of the full 12 by 12 Hamiltonian (B,M,n) as a function of the multiport phase angle ϕ

5.5.1 Discussion

As revealed earlier, there are two special cases of energy behaviour of the system when the multiport angle is set to $\pi/2$ or $3\pi/2$ which results in a two 6-fold degeneracy system or six 2-fold degeneracy system respectively.

However, for $\phi \neq \frac{k\pi}{2}(k \in \mathbb{Z}$, the system produces a system of four 2-fold degeneracies and eight distinct eigenvalues.

Eigenvalues with a value of $-\pi/2$ always produce an eigenstate that exhibits periodic amplitude behaviour among states (exception being $E = -\pi/2$ for the special case phase angles of $\pi/2, 3\pi/2$).

Other important behaviour include the energy jumps that occur at the following phase angles - $\pi/6, \approx 0.9272, \approx 2.2142, 5\pi/6$.

In the case of $\pi/6$, the twelve eigenvalues converged to π-multiple values on the unit

circle as the multiport phase angle gets closer and closer to $\pi/6$.

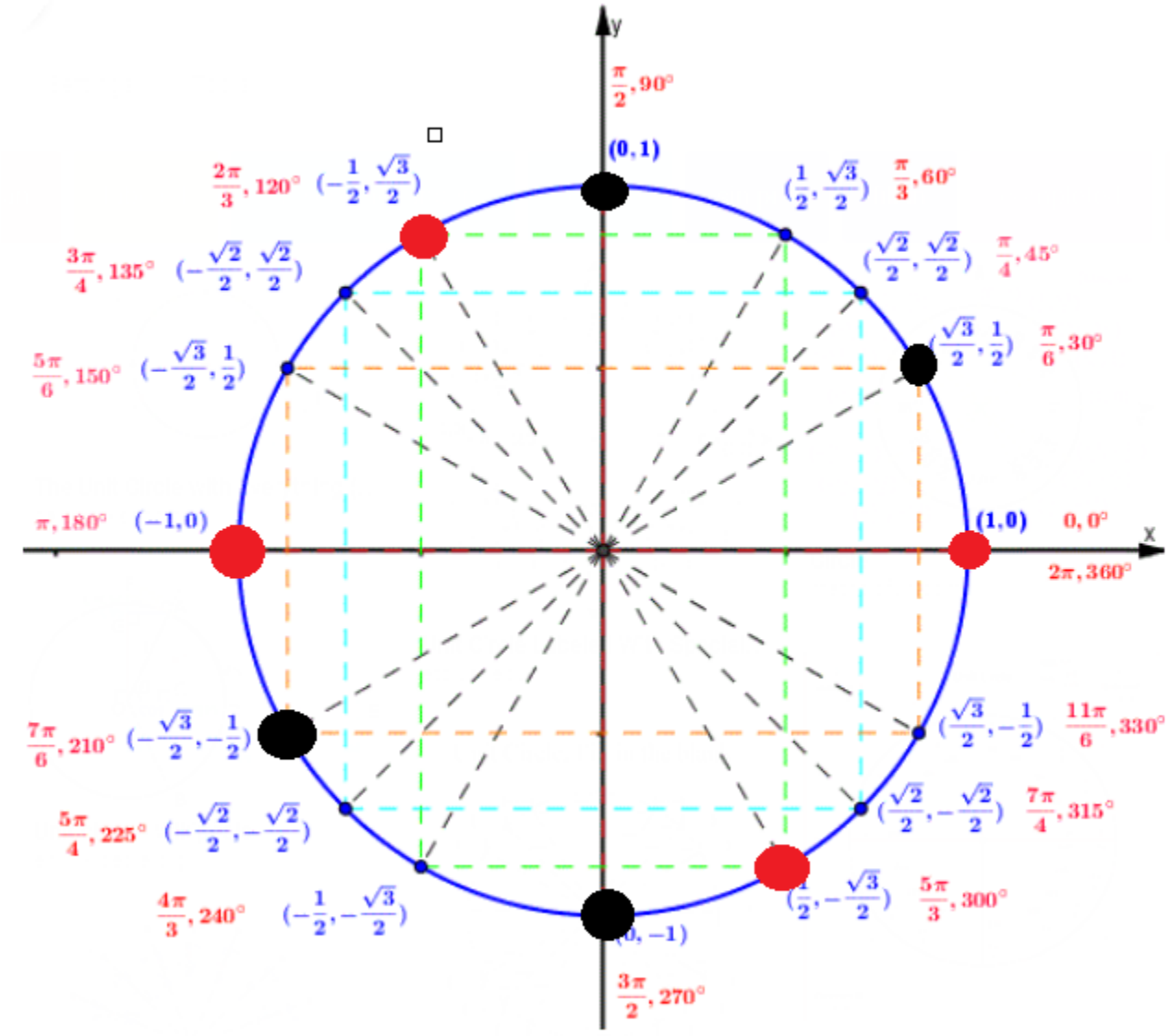

Figure 5·4: The eigenvalues the system converges as the multiport phase angle $\phi \to \pi/6$

Red circles denote energies that are 2-fold degenerate and the black circles are non-degenerate energies. It is evident from the convergence of the values before jumping, there's some periodic or cyclic behaviour going on with the energies. If the phase angle becomes $\pi/6$ then the eigenvalues themselves wrap around themselves and are

symmetric from each other when it comes positive and negative values.

For example, as $\phi \to \pi/6$ the values in the following eigenvalues $E_3 = -5\pi/6, E_4 = -\pi/2$ shift up when $\phi = \pi/$, we then see the value of $-5\pi/6, -\pi/2$ contained in E_1 and E_2.

5.6 Eigenspectrum of Reduced Hamiltonian

When we use the Hamiltonian that models the energy at the Bond Sites and Unit Cell position given by Eq. 4.36, we get a similar looking Eigenvalue spectrum to that of the full 12 by 12 Hilbert Space Hamiltonian earlier:

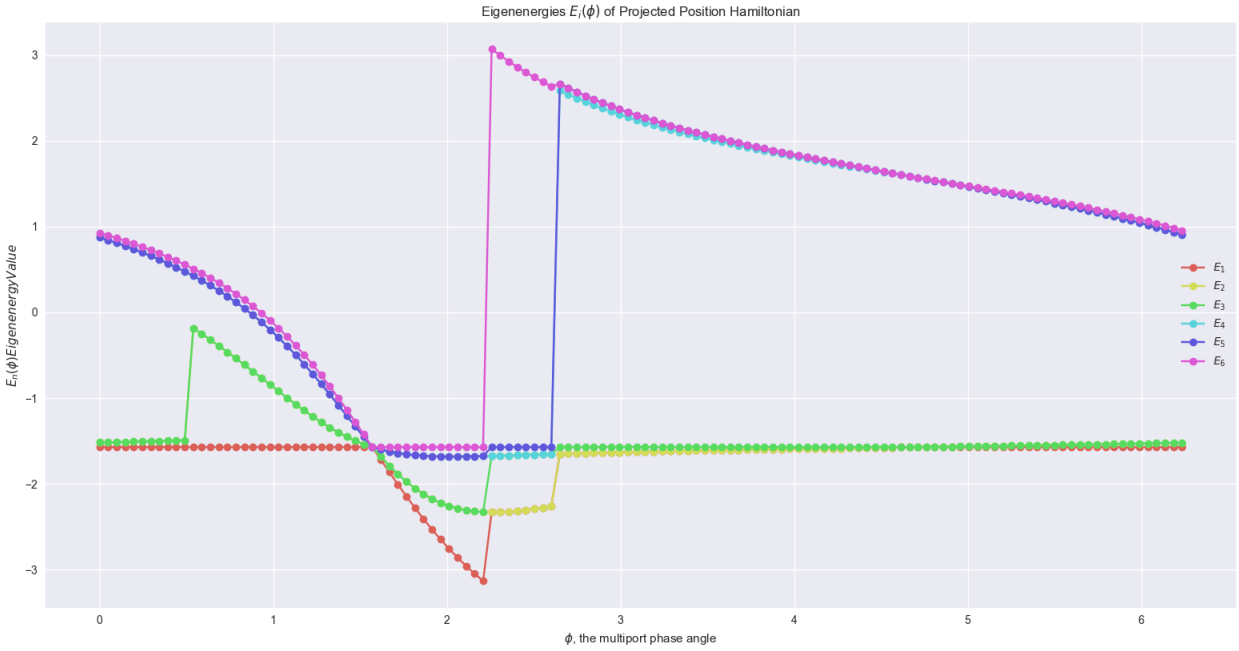

Figure 5·5: Eigenvalue/Eigenenergy spectrum of the projected Hamiltonian (B, n) as a function of the multiport phase angle ϕ

5.6.1 Discussion

The reduced model produces a system with characteristics more similar to that of a Benzene molecule. The Hamiltonian produces a set of two 2-fold degenerate energies

and two non-degenerate energies (total of 6 energies) which is analagous to that of the Benzene molecule which produces the same behaviour of degeneracies (see Appendix A.1 for more).

Just like the Full Hamiltonian model, this one produces the same special cases that occur for multiport phase angles of $\pi/2$ and $3\pi/2$.

For $\phi = \pi/2$, all 6 energies collapse down to a single energy level value of $-\pi/2$

For $\phi = 3\pi/2$, the 6 energies collapse to a pair of 3-fold degeneracies at values of $-\pi/2$ and $\pi/2$ respectively.

Eigenstates produced by the Reduced Model have a similar pattern to that of the Full Hamiltonian. Once again an energy value of $-\pi/2$ is always an eigenvalue for all ϕ and always produces an eigenstate with periodic behaviour for the probability amplitude except for phase angles of $\pi/2, 3\pi/2$ as shown below for a multiport phase angle of $\pi/6$

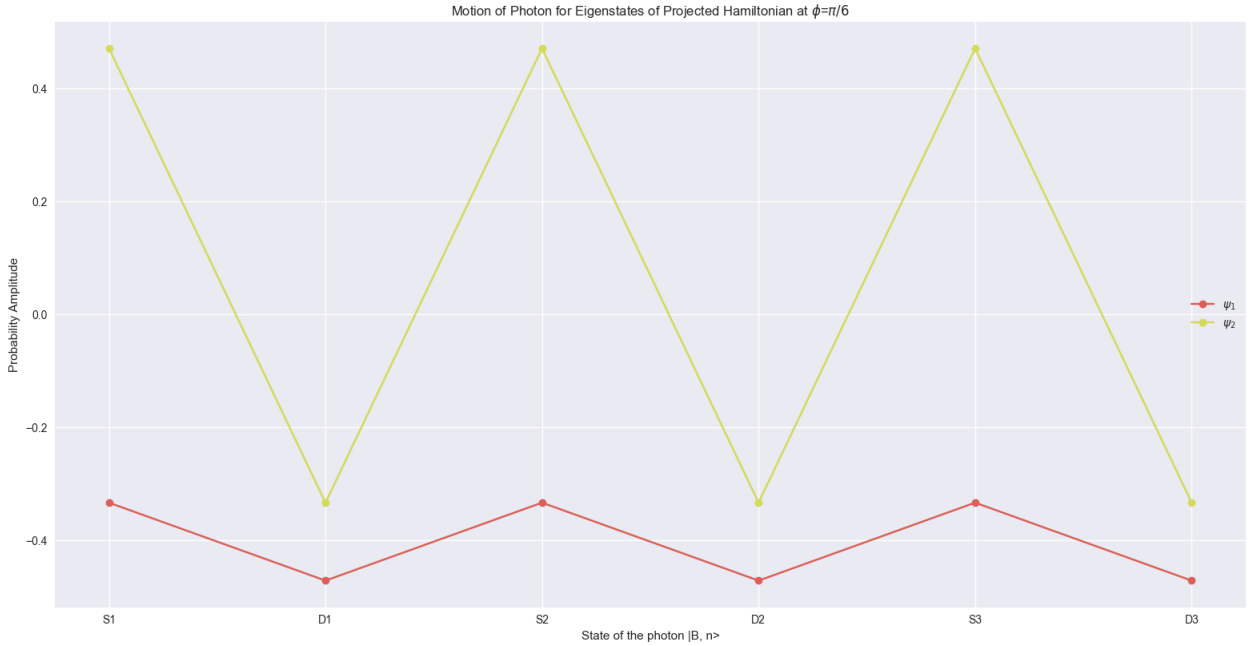

Figure 5·6: Probability Amplitude as a function of the state $|B, M, n\rangle$ of the Periodic Eigenstates for the associated Eigenvalues for a Hamiltonian solved with a multiport phase angle of $\pi/6$

ψ_1(red) represents $E = -\pi/2$ and ψ_2 represents $E = \pi/6$.

Periodic eigenstates appear for non-degenerate eigenvalues and all degenerate eigenvalues produce stated with mixed amplitude (no pattern).

The periodic amplitude shows symmetric probability of being within a specific bond site across unit cell jumps (i.e. $S1 \to S2, D2 \to D3$etc.) Energy jumps in this system occurs at three points of the system at $\pi/6$, $\approx 2.2142, 5\pi/6$ respectively. However, for $\phi = \pi/6$ only energy experiences a jump as opposed to the two occurrences.

Benzene exhibits energies with symmetry of the following approximations (see Appendix A.1 for Huckel Model)

$$E = \alpha - 2\beta, \alpha - \beta, \alpha + \beta, \alpha + 2\beta \tag{5.48}$$

Where α, β are parameters (note: this β is different than the one I defined in the model).

The positive-negative symmetry for the Huckel Model of Benzene does not occurs in the interval starting from the last energy jump at $5\pi/6$ which goes on until E_3 jumps at $\pi/6$. However, the spacing of the energies does not come close to that of the Model and are often within range of folding into 3-fold degeneracy as shown below for the reduced model evaluated at a multiport phase angle of $11\pi/6$

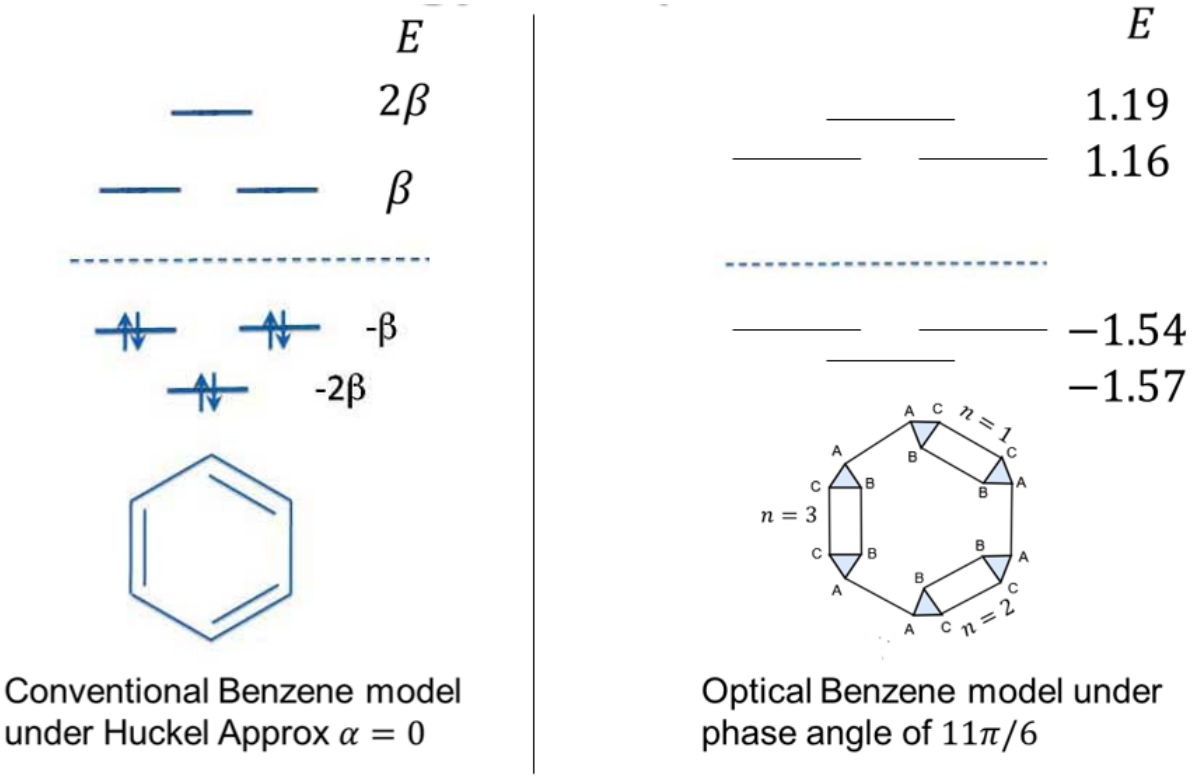

Figure 5·7: Energy Comparison of the Huckel Model of Benzene versus the Optical Benzene model under a phase angle of $11\pi/6$

Chapter 6

Conclusions

In this dissertation novel insight was earned through an application of Hamiltonian-based Photonic Quantum Information Processing. It was evident one can use linear optical devices and form complex characterized structures which can be put together to form physical models that represent atomic molecules in nature. Using this insight offers a new approach to tackling molecular modeling in the fields of Quantum Chemistry and Quantum Computing. A summary of results and future approaches is down below.

6.1 Summary of Work and future directions

Using a network of directionally-unbiased optical multiports, we are able to construct a characterizable system that mimics one that of a simple molecule which in this case was Benzene. Even though the results didn't have the accurate spacing that is synonamous to the Huckel Model, it provided the same symmetry and behaviour and thats an important feature to get out of this. Apart from that, insight was obtained in the behaviour of photons in a closed network of optical multiports such as its periodic nature, how it moves in the system, and for quantum walks. With additional pertubation and correction. one could achieve even closer modeling of the molecule. Given that the Huckel model is also just a simple approximation of aromatic hydrocarbons and ignores certain atomic interactions, it is interesting to note how our system of optical elements can produce similar simple molecular behaviour modeling.

Further research can be made into creating more complex multiport networks. One may be able to study the entangled quantum walk dynamics on complex multiport models which are similar to graphical models. Even using the existing benzene molecule, one may be able to create other benzene-like chemical compounds or benzene-dependent molecules and characterize those. Eventually, it would be feasible to scale down these systems into an optical chip system and do more complex information processing and modeling. The biggest constraint would be the experimental realization of this work which requires additional designing, more parameters, and extensive testing. Nevertheless, multiport networks are efficient and versatile and offer a new approach to tackling quantum chemistry and quantum computing systems. I leave research for more complex networks and other means of mathematics as a topic for future researchers.

Appendix A

Appendices

A.1 Huckel

The Huckel Approximation Method is based off the Huckel Molecular Orbital Theory model which uses the π-orbitals of a conjugated system to approximate the Hamiltonian and its corresponding eigenenergies. The π-orbitals turn out to be the highest occupied orbitals with the σ-orbitals being more strongly bound. As a result, the forming and breaking of bonds from resonance structures is easier to describe with the breaking and making of π bonds than σ-bonds.

The approximation of Huckel Theory can be outlined in Molecular Orbital Theory

1. **Define a basis of atomic orbitals** Since the Huckel Model is taking into account π_z orbitals, we create MOs as a linear combination of p_z orbitals. Assuming N carbon atoms, each contributing a p_z orbital then we write the μth MOs as:
$$\pi^\mu = \sum_{i=1}^{N} c_i^\mu p_z^i \tag{A.1}$$
2. **Compute relevant matrix representations** We use big approximations to make the algebra easier. We have two matrices **H** and **S** which involve integrals

between p_z orbitals on different atoms:

$$H_{ij} = \int p_z^i \hat{H} p_z^j d\tau \tag{A.2}$$

$$S_{ij} = \int p_z^i p_z^j d\tau \tag{A.3}$$

The first approximation is that p_z orbitals are **orthonormal**

$$S_{ij} = \begin{cases} 1 & i = j \\ 0 & i \neq j \end{cases} \tag{A.4}$$

Since **S** represents an identity operator, we reduce our generalized eigenvalue problem to a normal eigenvalue problem

$$\mathbf{H} \cdot \mathbf{c}^\alpha = E_\alpha \mathbf{S} \cdot \mathbf{c}^\mu \rightarrow \mathbf{H} \cdot \mathbf{c}^\mu = E_\mu c^\mu \tag{A.5}$$

The second approximation is to assume that any Hamiltonian integrals **vanish** if they involve atoms i, j that are not nearest neighbors because if p_z orbitals are far apart, there is little spatial overlap leading to the integrand being near zero everywhere. Note that diagonal terms must be the same as it involves the average energy of an electron in a carbon p_z orbital:

$$H_{ii} = \int p_z^i \hat{H} p_z^i d\tau = \alpha \tag{A.6}$$

Since it describes the energy of an electron on a single carbon, α is the sometimes referred to as the on-site energy. Any two nearest neighbours will produced a constant

$$H_{ij} = \int p_z^i \hat{H} p_z^i d\tau = \beta \tag{A.7}$$

The nearest neighbor approximation is good as long as the C-C bond lengths in the molecules are all nearly equal. If there is any significant bond length

alternation, then this approximation can be relaxed to allow β to depend on the C-C bond distance. β will allow us to describe the electron delocalization that comes from multiple resonance structures. There is often debate for the right parameters, usually they are taken to be $\alpha = -11.2\text{eV}$ and $\beta = -0.7\text{eV}$

3. **Solve generalized eigenvalue problem**

4. **Occupy orbitals according to the stick diagram** We note that from Np_z orbitals , we obtain $N\pi$ orbitals. Each carbon has one free valence electron to contribute, for a total of N electrons that will need to be accounted for (assuming the molecule is neutral). If one accounts spin, then there are $N/2$ occupied MO's and $N/2$ unoccupied ones. For the ground state, we of course occupy the lowest energy orbitals.

5. **Compute the energy** Since it's a approximate form of MO Theory, Huckel uses the non-interacting electron energy expression:

$$E_{tot} = \sum_{i=1}^{N} E_i \tag{A.8}$$

Where E_i are the MO eigenvalues determined in the third step.

In the context of a benzene molecule let's try this out

1. Represent the MOs as a linear combination of 6 p_z orbitals

$$\psi^\mu = \sum_{i=1}^{6} c_i^\mu c_i^\mu p_z^i \rightarrow \mathbf{c}^\mu = (c_1^\mu, c_2^\mu, c_3^\mu, c_4^\mu, c_5^\mu, c_6^\mu)^T \tag{A.9}$$

2. The Hamiltonian following the rules becomes the following

$$H = \begin{pmatrix} \alpha & \beta & 0 & 0 & 0 & \beta \\ \beta & \alpha & \beta & 0 & 0 & 0 \\ 0 & \beta & \alpha & \beta & 0 & 0 \\ 0 & 0 & \beta & \alpha & \beta & 0 \\ 0 & 0 & 0 & \beta & \alpha & \beta \\ \beta & 0 & 0 & 0 & \beta & \alpha \end{pmatrix} \tag{A.10}$$

3. Solving the eigenvalue problem we get the 4 distinct energies (total 6 - two 2-fold degeneracies and 2 non-degeneate values)

$$E_1 = \alpha + 2\beta \tag{A.11}$$

$$E_2 = E_3 = \alpha + \beta \tag{A.12}$$

$$E_4 = E_5 = \alpha - \beta \tag{A.13}$$

$$E_6 = \alpha - 2\beta \tag{A.14}$$

4. The Corresponding EIgenvectors are then

$$c^1 = \frac{1}{\sqrt{6}} \begin{pmatrix} 1 \\ 1 \\ 1 \\ 1 \\ 1 \\ 1 \end{pmatrix} c^2 = \frac{1}{\sqrt{12}} \begin{pmatrix} 1 \\ 2 \\ 1 \\ -1 \\ -2 \\ -1 \end{pmatrix} c^3 = \frac{1}{\sqrt{4}} \begin{pmatrix} 1 \\ 0 \\ -1 \\ -1 \\ 0 \\ 1 \end{pmatrix} \tag{A.15}$$

$$c^4 = \frac{1}{\sqrt{4}} \begin{pmatrix} 1 \\ 0 \\ -1 \\ 1 \\ 0 \\ -1 \end{pmatrix} c^5 = \frac{1}{\sqrt{12}} \begin{pmatrix} 1 \\ -2 \\ 1 \\ 1 \\ -2 \\ 1 \end{pmatrix} c^6 = \frac{1}{\sqrt{6}} \begin{pmatrix} 1 \\ -1 \\ 1 \\ -1 \\ 1 \\ -1 \end{pmatrix} \tag{A.16}$$

5. Given that there are 6 π electrons in Benzene, the first 3 MOs are doubly occupied.

6. The total Huckel Energy is then

$$E = 2E_1 + 2E_2 + 2E_3 = 6\alpha + 8\beta \tag{A.17}$$

A.2 Matrix Logarithm

Unlike the scalar logarithm, there are no naturally-defined bases for the matrix logarithm, therefore the matrix logarithm is taken to be the natural logarithm. In general there may be an infinite number of matrices B satisfying $e^B = A$, these are known as the logarithms of A.

The matrix logarithm like the scalar natural log, can be defined as a power series when A is a square matrix and $||I - A||_F < 1$ where $||\cdot||_F$ is the Frobenius matrix norm. The logarithm this formula provides is known as the principle logarithm of A:

$$\log(A) = -\sum_{k=1}^{\infty} \frac{(I-A)^k}{k} = log(I+X) = \sum_{k=1}^{\infty} \frac{(-1)^{k+1}}{k} X^k \tag{A.18}$$

Since the series expansion does not converge for all A, it is not a global inverse function for the matrix exponential. In particular $e^{\log A} = A$ only holds for $||I - A||_F < 1$ and $\log(\exp A) = A$ only holds for $||A||_F < 2$.

There are other ways of calculating it such as a contour integral. An analytical function f of a square matrix A can be represented as

$$f(A) = \frac{1}{2\pi i} \oint_{\Gamma} f(z)(zI - A)^{-1} dz \tag{A.19}$$

Where Γ is a closed contour lying in the region of analyticity of f and winding once around the spectrum $\sigma(A)$ in the counterclockwise directin.

A.3 Engineering Requirements

Component	*Directionally-unbiased Optical Multiport (Triangular 3-port)*
Function	Simulation of an electron system through photons undergoing quantum walks in a physical space
Objective	Photons can leave/enter from the same port and go to any of the other ports, allowing for better random walks and scattering.
Constraints	The coherence length (propagation distance for which a coherent wave stays at a degree of coherence) of the photons. The coherence time for this multiport is found to be $\approx$ 1ps with a coherence length of about 10^{-4}m. Ample coherence of the photons of the is required to have a well-defined phase during the walk. The number of steps for which coherence is able to be maintained will limit the accuracy of the results.

Component	*Beam Splitter*
Function	Split an incident light beam (i.e. laser) into two or more beams which may or may not have the same optical power.
Objective	The inclusion of a partially reflective mirror or some other medium at some angle of incident to split the beam. If the beam splitter is directionally-unbiased, there is reversibility (i.e. photons that enter through the same port, have the option to exit out back the same port).
Constraints	Angle of incident must be adjusted accordingly as well as the reflectivity dependence on the polarization state of an incident beam.

Component	*Fibers (Lossless, Optical Circulator)*
Function	Transmit light between two ends (Control optical signals/photons from one end to the next exit port in the circulator)
Objective	Allows optical communication with low loss of power (dB)
Constraints	Insertion loss leads to reduction in optical power.

Component	*Optical Mirrors*
Function	To reflect light
Objective	Contain a type of reflective coating to ensure high reflectivity of a required wavelength or wavelength range.
Constraints	Specific coatings require specific thermal expansion coefficients as well as the possibility of partial transmission of light.

Component	633nm *Long Coherent Length Laser*
Function	To deliver a incident beam of photons into a optical system/circuit.
Objective	A stream of photons that can circulate around a optical circuit with a long coherence length so that photon states will be distinguishable.
Constraints	The coherence length (propagation distance for which a coherent wave stays at a degree of coherence) of the photons.

References

Adami, C. and Cerf, N. J. (1999). Quantum computation with linear optics. In Williams, C. P., editor, *Quantum Computing and Quantum Communications*, pages 391–401, Berlin, Heidelberg. Springer Berlin Heidelberg.

Aharonov, Y., Davidovich, L., and Zagury, N. (1993). Quantum random walks. *Phys. Rev. A*, 48:1687–1690.

Aspuru-Guzik, A. and Walther, P. (2012). Photonic quantum simulators. *Nature Physics*, 8:285–291. n/a.

Bian, Z.-H., Li, J., Zhan, X., Twamley, J., and Xue, P. (2017). Experimental implementation of a quantum walk on a circle with single photons. *Phys. Rev. A*, 95:052338.

Blatt, R. (2012). Quantum information processing and quantum simulations with trapped ions. *Research in Optical Sciences*, page QM2A.1.

Broome, M. A., Fedrizzi, A., Lanyon, B. P., Kassal, I., Aspuru-Guzik, A., and White, A. G. (2010). Discrete single-photon quantum walks with tunable decoherence. *Phys. Rev. Lett.*, 104:153602.

Childs, A. M., Gosset, D., and Webb, Z. (2013). Universal computation by multiparticle quantum walk. *Science*, 339(6121):791–794.

Das, A. and Chakrabarti, B. K. (2008). Colloquium. *Rev. Mod. Phys.*, 80:1061–1081.

Feldman, E. and Hillery, M. (2004). Scattering theory and discrete-time quantum walks. *Physics Letters A*, 324(4):277 – 281.

Feynman, R. P. (1982). Simulating physics with computers. *International Journal of Theoretical Physics*, 21(6):467–488.

Fitzpatrick, Casey, A. (2017). High-dimensional quantum information processing with linear optics.

Gerry, C. and Knight, P. (2005). *Introductory Quantum Optics*. Cambridge University Press.

Kempe, J. (2003). Quantum random walks: An introductory overview. *Contemporary Physics*, 44(4):307–327.

Kok, P., Munro, W. J., Nemoto, K., Ralph, T. C., Dowling, J. P., and Milburn, G. J. (2007). Linear optical quantum computing with photonic qubits. *Rev. Mod. Phys.*, 79:135–174.

McHale, C. M., Zhang, L., and Smith, M. T. (2012). Current understanding of the mechanism of benzene-induced leukemia in humans: implications for risk assessment. *Carcinogenesis*, 33(2):240–252.

Nielsen, M. A. and Chuang, I. L. (2011). *Quantum Computation and Quantum Information: 10th Anniversary Edition*. Cambridge University Press, New York, NY, USA, 10th edition.

Paraoanu, G. S. (2014). Recent progress in quantum simulation using superconducting circuits. *Journal of Low Temperature Physics*, 175(5):633–654.

Ravindran, J., Prasad, S., and Aggarwal, B. (2009). Curcumin and cancer cells: How many ways can curry kill tumor cells selectively? 11:495–510.

Schreiber, A., Cassemiro, K. N., Potoček, V., Gábris, A., Mosley, P. J., Andersson, E., Jex, I., and Silberhorn, C. (2010). Photons walking the line: A quantum walk with adjustable coin operations. *Phys. Rev. Lett.*, 104:050502.

Simon, D. S., Fitzpatrick, C. A., and Sergienko, A. V. (2016). Group transformations and entangled-state quantum gates with directionally unbiased linear-optical multiports. *Phys. Rev. A*, 93:043845.

Turing, A. M. (1937). On computable numbers, with an application to the entscheidungsproblem. *Proceedings of the London Mathematical Society*, s2-42(1):230–265.

Venegas-Andraca, S. E. (2012). Quantum walks: a comprehensive review. *Quantum Information Processing*, 11(5):1015–1106.

THANK YOU

Sonam Ghosh